The International Journal of Advanced Manufacturing Technology (2020) 107:1959–1982
https://doi.org/10.1007/s00170-020-05027-0

ORIGINAL ARTICLE

Modeling of the laser powder–based directed energy deposition process for additive manufacturing: a review

Xiaoyi Guan[1] · Yaoyao Fiona Zhao[1]

Received: 27 September 2019 / Accepted: 27 January 2020 / Published online: 12 March 2020

Abstract

Laser powder–based directed energy deposition (DED) is a specific additive manufacturing process that offers an effective way to fabricate parts via simultaneous delivery of powders and laser beam. It has been developing greatly in the recent decades and being widely used for manufacturing, prototyping, and repairing. Complex physical events take place during the manufacturing process and have great impacts on its overall performance. To build high-quality parts through the laser powder–based DED process, its physical insights and process parameters need to be understood and optimized, for which modeling provides an efficient way. This article gives a review of the modeling work for the laser powder–based DED process, in which the models developed for powder stream and its interaction with laser beam, melt-pool, and bulk heating are discussed in detail. Different modeling approaches and methods towards overall and specific physical processes of the laser powder–based DED are analyzed and compared. Suggestions towards the modeling are also given at the end.

Keywords Directed energy deposition · Modeling · Laser beam · Powder stream · Melt-pool and bulk heating

1 Introduction

Additive manufacturing (AM), as a burgeoning manufacturing method, has evolved greatly in the past several decades [1, 2]. The fabrication process of AM was defined by the American Society for Testing and Materials (ASTM) International as the process of bonding materials, usually layer upon layer, to build parts based on three-dimensional (3D) computer-aided design (CAD) model, which differs from the conventional subtractive and formative manufacturing methodologies [3]. As one of the AM processes, directed energy deposition (DED) [3] has been broadly used in product manufacturing, especially in metallic AM [4–6].

During DED process, focused energy source and material are fed onto desired regions simultaneously. The feeding material gets melted almost simultaneously along with part of the pre-deposited layers or substrate, which creates the so-called melt-pool containing liquid material. Then, in a very short time scale, the melted material solidifies and bonds with pre-deposited material or substrate, which enables the building of new layers. Laser [7] or electron-beam [8, 9] is frequently used as energy source in DED process. DED machines can accept powder [10], wire [11], or both as feeding material. Comparison between these two feeding methods was done by Syed et al. [12] and the potential combination of these two material feeding methods was investigated by Syed et al. [13].

For laser powder–based DED, also known as laser powder deposition (LPD) [14], powders are injected from a coaxial or multi-jet nozzle onto the focus region with the aid of carrier and/or shielding gas to enhance deposition efficiency and to minimize potential oxidation (if inert gas is used). Wire-based DED sometimes can outperform LPD in some aspects such as process efficiency and surface quality. However, powder delivery can be better controlled compared with wire feeding machine and hence more complex and accurate fabrication can be achieved through powder-based machines. Moreover, LPD offers a great amount of diversity and convenience and enables the fabrication of parts with customized features and complex geometries. Multiple powder sources can be utilized by LPD to build functionally graded parts (e.g., [15–17]). LPD has also been used for repairing (e.g., [18–20]) and cladding operations (e.g., [21, 22]). Concepts of LPD emerged decades ago such as the laser engineered net shaping (LENS) process [23].

✉ Yaoyao Fiona Zhao
yaoyao.zhao@mcgill.ca

[1] Department of Mechanical Engineering, McGill University, Montreal, Quebec, H3A 0C3, Canada

Note that LPD will be used in the remaining article instead of laser powder–based DED for simplicity.

To successfully build parts by LPD, its physical insights need to be clearly understood. A typical LPD process can be seen in Fig. 1, in which complex physical events take place. Powders are blown from nozzles and carried by gas to desired deposition area. During flight, they interact with the laser beam and are heated due to laser irradiation. Laser beam is attenuated by the powder stream and then irradiates onto the surface of melt-pool and substrate. Melt-pool connects the blown powders, deposited layers, and/or substrate. Its dynamical and thermal behaviors deeply impact the quality of the built parts. Melt-pool absorbs the energy from laser irradiation but also loses it through heat conduction, convection, and radiation. In melt-pool, super-heating generally occurs and temperature gradient is large. For example, as shown in Fig. 2, the temperature gradient is as large as 160 K/mm, which suggests significant heat transfer and thermal-driven flow. Injected powder stream carries mass, momentum, and energy, which also contributes to the transport phenomena of melt-pool. Generally, the length scale of melt-pool is on the order of 1 mm. Capillary and thermo-capillary forces strongly influence the transport behaviors and hence the shape of melt-pool. Phase change taking place at the boundary of the melt-pool, including melting, solidification, and evaporation, and the accompanying latent heat are also relevant to the transport phenomena of melt-pool. The presence of the mushy zone due to melting and solidification near the interface between liquid and solid in the LPD process of alloying material also influences the dynamics of melt-pool. Located near the melt-pool, the heat affected zone (HAZ) goes through significant heat transfer and related mechanical behaviors due to large temperature gradient. Also, the repetitive laser scanning in multi-layer and/or multi-track induces cyclic heating in HAZ. Heat transfer phenomenon exists almost in every stage of LPD process and the bonding of layer to layer and layer to substrate is largely determined by effective energy transfer. Comprehensive reviews of the LPD process have been given by Thompson et al. [24] and Shamsaei et al. [25].

Moreover, the optimization of process parameters is necessary for better performance of LPD. However, for different designs, materials, and operating environments, appropriate process parameters vary significantly because of complex phenomena occurring in LPD. Kahlen and Kar [27] listed a large number of process parameters that could impact the manufacturing process. Thus, to achieve desired qualities, it is essential to build quantitative relationships between the process parameters and the interested properties of final parts such as porosity, residual stress, and microstructure. Modeling of LPD offers a way to virtually build parts and to find optimal process parameters with lower cost, which has been conducted extensively and important progress has been made.

A review of the modeling for LPD process will be given in the following sections. As LPD involves complex physical processes, its modeling work will be divided and discussed in separate sections. General considerations of the modeling of LPD will be discussed first in Section 2. Then, the modeling work of powder stream including its interaction with laser will be reviewed in Section 3. Models for melt-pool and bulk heating will be discussed together in Section 4. In this section, mechanical analysis such as

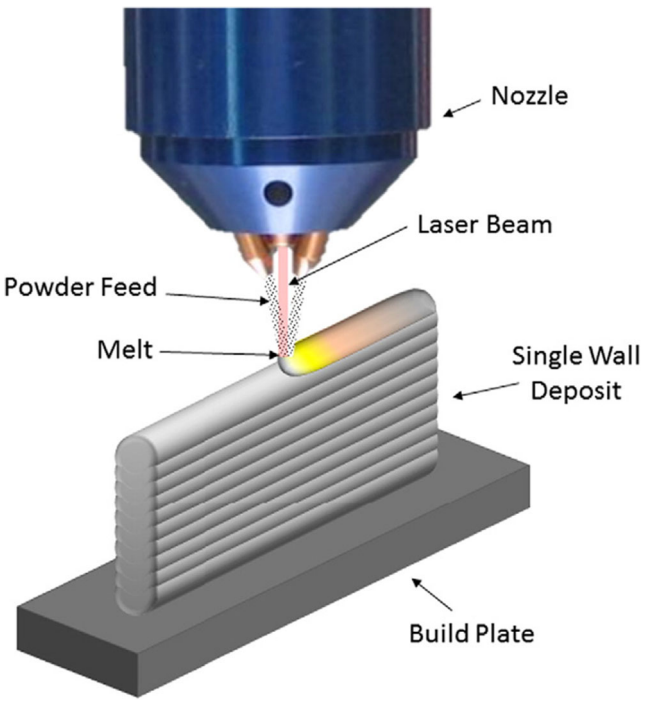

Fig. 1 A typical LPD process [17]

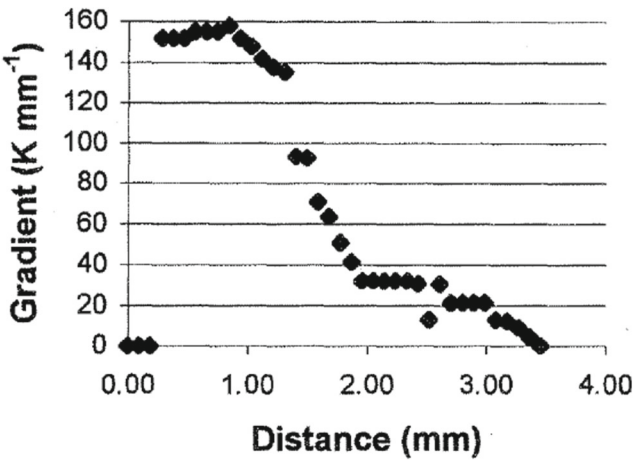

Fig. 2 Temperature gradient across the melt-pool in LENS process for stainless steel 316 [26]

residual stress evaluation will also be covered if presented in the reviewed literature but without detailed discussion. Pinkerton [28] has given a brief review on the modeling of LPD, but in this paper the focus will be put on the details and recent advancements of the models presented in reviewed literature especially on the modeling of powder stream, melt-pool, and bulk heating. Note that the microstructural modeling of LPD will not be discussed in this paper. Discussion and conclusions of the modeling work for LPD will be given at the end.

2 Modeling of laser powder deposition

For such a complex manufacturing process like LPD, an integrated modeling framework is needed to obtain the thermal, mechanical, and material performance and to understand its physical insights [29, 30]. A modeling flow chart for LPD was summarized and shown in Fig. 3, from which it can be seen that generally there are three coupled components in the modeling of LPD: powder stream and laser interaction; melt-pool and bulk behaviors; microstructural modeling.

First, the powder stream dynamics and its interaction with laser beam need to be modeled. This part delivers the attenuated laser beam and the profile of powder stream including mass, momentum, and energy, which will impact the transport behaviors of melt-pool and bulk heating. Second, the physical events of melt-pool, such as transport phenomena and phase changes, need to be carefully modeled because it connects the whole building process. It accepts the outcomes of powder stream model and outputs what will be used in the modeling of bulk heating, potential mechanical analysis and microstructural modeling. The model for transport phenomena in melt-pool needs the results of bulk heating as boundary conditions and vice versa. Actually the powder stream and melt-pool processes are also coupled together but many reviewed models, especially numerical models, treat them separately mainly due to complex modeling work and high computational cost. Meanwhile, mechanical analysis can also be included with the bulk heating due to the thermal strains during deposition process. Finally, the modeling of microstructure during solidification and repetitious scanning is another major part in the modeling framework, which, however, will not be discussed in this paper. The majority of the existing literature delves into one or two parts of the process and makes simplified assumptions for other parts as LPD consists of extensive physical phenomena and a complete simulation model is rather complex and expensive.

As shown in Fig. 3, the modeling of LPD needs many inputs that are critical to the performance of the built model. The physical properties of materials and their relationships with the physical variables such as temperature need to be provided correctly. However, some of these relationships are still not clear for certain materials and simplifications such as constant or linear relationships are often made. Furthermore, process settings and parameters should be identified clearly especially in numerical models. Laser type, power distribution, beam diameter, scanning pattern, and speed need to be ready to use. Nozzle settings such as nozzle geometry and stand-off distance are important to the entire process as they greatly impact the powder deposition. Substrate characteristics also need to be correctly fed into

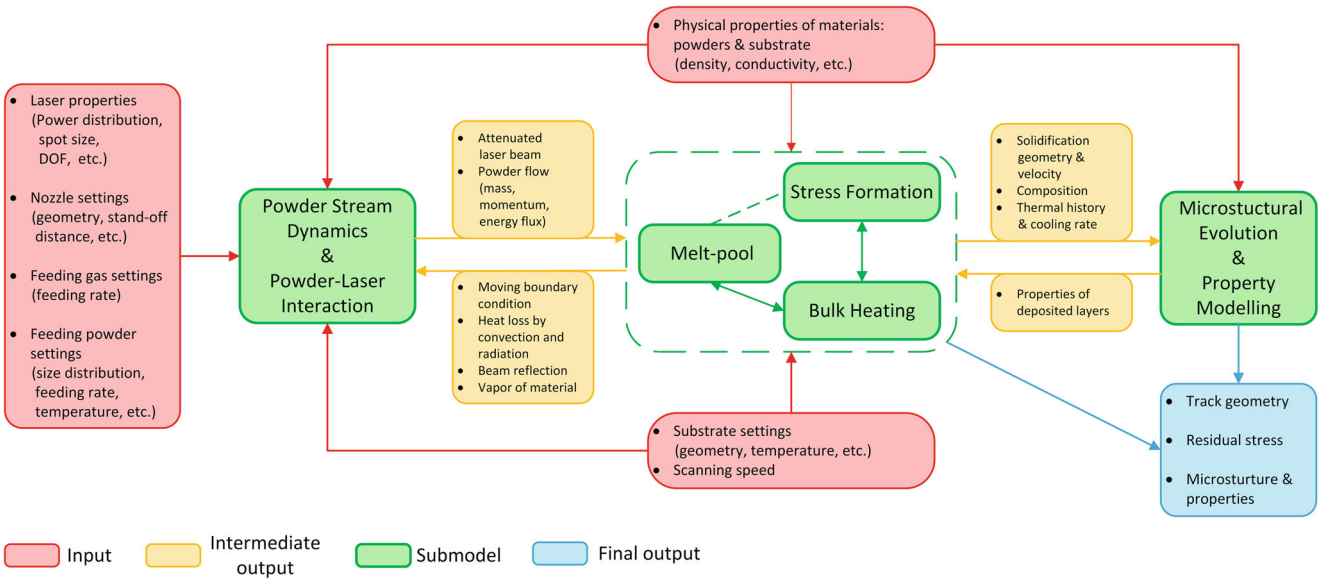

Fig. 3 Flow chart of modeling for LPD

the model. The model of LPD produces results such as thermal profile and history, track geometry, residual stress, and microstructures, which can be used as the criterion of process performance and the targets of optimization.

Generally, there are three approaches for modeling LPD overall: analytical, numerical, and hybrid. In analytical approach, basic conservation laws are respected but due to transient and complex physical phenomena, highly simplified assumptions need to be made towards powder stream, melt-pool, and bulk heating [31]. Advantages of this approach are obvious for it does not require high computational power and preprocessing work such as meshing in numerical models. But due to the high complexity of physics involved in LPD, this kind of models has many constraints such as physical inconsistency, which limit its usage. For numerical approach, models based on conservation equations are developed and solved numerically [32]. Numerical models generally adopt fewer simplifications and hence can deliver physically more realistic results. But the modeling work and computational cost involved to solve the coupled numerical model for powder stream, melt-pool, and bulk heating is quite high. A compromising approach, hybrid approach, is extensively used in the reviewed literature, where the powder stream process is decoupled from the rest [33] and modeled analytically. Then, the results of powder stream from analytical model are fed into the numerical model for melt pool and bulk heating.

3 Modeling of powder stream and its interaction with laser beam

Powder stream and its interaction with laser are very complex due to the presence of two-phase turbulent flow, laser attenuation and radiative heat transfer. It can be seen from Fig. 3 that the powder stream process and its interaction with laser beam are the starting point of LPD process. The powder flow and the laser beam after attenuation have great impacts on the following physical processes such as melt-pool. To obtain the laser beam after attenuation and the mass, momentum, and energy flux of powder stream, analytical and numerical models have been established.

Due to the high complexity involved, various assumptions are adopted in both analytical and numerical models. The collisions of particles are frequently neglected to simplify the problem due to the low volume fraction of powder particles. Moreover, powders are usually treated as lumped capacity because of low Biot number [34]. The shape of powder particles is usually assumed to be spherical or non-spherical with fixed shape factor. The powder size is often assumed to have certain distribution such as uniform or Rosin-Rammler [35]. To describe the energy transfer of laser irradiation on powders (or melt-pool), the absorption coefficient based on Hagen-Rubens relationship [36] or Bramson's equation [37] is widely used and it is generally assumed to be uniform and constant. Laser attenuation is often assumed to be proportional to the area of the particles projected to the beam in agreement with Mie's theory [38] or to obey the Beer-Lambert law [39], both of which result in similar mathematical forms. The shadowing effect of particles is generally neglected when it comes to the modeling of laser irradiation on powders [40].

3.1 Analytical models

Analytical models for powder stream dynamics and its interaction with laser beam have been developed based on the related conservation laws and simplified assumptions such as pre-defined powder concentration and movement models. The most frequently used assumption is the spatial Gaussian distribution of laser power. Meanwhile, the powder concentration is also generally assumed to be Gaussian, which has been experimentally validated [41]. Stationary gas flow field, uniform powder size distribution, spherical powder shape, and collimated laser beam are generally assumed if used. Powder concentration, laser beam after attenuation, and thermal profile of powder stream have been investigated the most mainly because they serve as inputs for subsequent models.

Lin [42] developed a two-stage analytical model considering the stages before and after the converging point of powder stream. Before converging point, a bi-modal Gaussian distribution was used while a normal Gasussian distribution was applied after the focus point. Mean concentration was assumed to be inversely proportional to the stream width that depends on the initial stream width and stream angle. Pinkerton and Li [43, 44] modified this model by directly using a Gaussian distribution after merging point, where its corresponding stream can be extrapolated back to the surface of the nozzle tip. Meanwhile, the Gaussian distribution before the focus point was constructed in the same way. Yang [45] analytically developed a Gaussian model based on an existing movement model to predict the spatial concentration and volume fraction of powder stream in the regions after converging point.

The mode of powder concentration was also studied in LPD process with multiple nozzles. Chew et al. [46] developed a powder-laser interaction model for triple-nozzle LPD, where three separate Gaussian distributions were used for each of the streams and after converging simple summation was applied. Tan et al. [47] developed a model with pre-defined stream shape and Gaussian distribution assumption to describe the mass concentration of the powder stream in different nozzle settings such as single, double, or four symmetric powder nozzles. A homogeneous transformation was used by Wu et al.

[48] to transform the Gaussian powder distribution of individual nozzle to the global coordinate frame and then a summation was applied to obtain the combined distribution. Stankevich et al. [49] used a Gaussian distribution to represent the powder concentration, through which powder capture coefficient was calculated in single and three nozzle systems. An imitated circle or ellipse was presented to mimic melt-pool surface.

Due to the scattering effects of powder stream, laser beam is attenuated. Related models were constructed to describe such phenomenon as the attenuated laser beam not only affects the thermal profile of powder stream but also the melt-pool process. Frenk et al. [50] built a model to calculate the attenuated laser power based on the Mie's theory for the scattering of particle cloud, where the attenuated energy is proportional to the effective visible area of powder stream. The mathematical formulation can be seen as follows [50]:

$$P_a = P[1 - exp(-\sigma_{ext} N_p l)] \tag{1}$$

where P_a is the laser power attenuated by powder stream; P is the original laser power; σ_{ext} is the extinction coefficient; N_p is the power concentration and l is the traveling distance of laser beam. This type of model has been widely used (e.g., [33, 51, 52]). Similar strategy dealing with laser attenuation was used by Pinkerton [53] to compute the intensity of laser beam after attenuation, where a linear relation between the projected area of powders on the beam and its attenuation was adopted.

Beer-Lambert law was also applied to account for laser attenuation by Lin [42] and its underlying physical consideration is the same as the models discussed before. This type of model adopting the Beer-Lambert law to analytically describe the powder-laser interaction was used extensively [54–57]. Chew et al. [46] considered not only the attenuation from Beer-Lambert law but also the energy required for powder heating and they were both subtracted from the laser heat flux.

Liu et al. [40] developed an analytical model to calculate the attenuated laser power with the consideration of beam convergence and divergence, which was rare in the analytical models considering laser attenuation. But the waists of laser beam and powder stream were assumed to coincide with each other and have a length of zero. Two submodels were built for regions before and after the waist point. The attenuation of laser beam was assumed to be proportional to the total visible area of powders at each cross-section plane of powder stream, which brings the attenuated laser power at desired planes by integration. However, only the total attenuated laser power can be obtained through this model.

Moreover, thermal analysis towards powder stream has been included in some analytical models. The majority of them are iterative models constructed based on energy conservation laws that can be seen in Section 3.2. Energy gained from laser beam are generally included because of its dominant role in powder heating process. Heat loss by forced convection was also included as an improvement [51]. Later, liquid fraction evolution and related heat transfer due to latent heat were added to enrich the physical details [56, 57]

From the above discussion, it can be found that analytical models have to make some over-simplified assumptions especially towards powder stream structure such as concentration model or pre-defined movement model, which are by no meas universal in LPD process. As for laser attenuation and thermal analysis of powder stream, various models have been built, which, however, cannot perform well without valid results of powder structure and movement. Nevertheless, analytical models for powder stream and its interaction with laser beam are widely used in the popular hybrid modeling approach for modeling LPD.

3.2 Numerical models of powder stream

Numerical methods are used extensively to calculate the dynamics of powder stream and its interaction with laser beam. Starting from the governing equations for the continuum phase of gas and the discrete phase of powder particles, the two-phase turbulent flow can be modeled numerically. To couple gas flow and powder stream, two methods are generally used, i.e., one-way or two-way coupling methods.

The one-way coupling method simply decouple the two models by first solving gas flow without considering the impacts of powder particle on gas field and then calculate powder stream based on the obtained gas field. The two-way coupling method computes the gas flow field and trajectories of powder stream by alternatively solving the governing equations of each phase until convergence. Meanwhile, numerical models towards the dynamics of powder stream were built with or without considering the wall effects such as substrate, pre-deposited layers, and powder feeder. Along with dynamic analysis, thermal modeling including laser attenuation can also be conducted.

Conservation equations of mass and momentum, as shown in Eqs. 2 and 3, are generally solved to describe the gas flow in powder stream through computational fluid dynamics (CFD) techniques such as finite volume method (FVM) [58].

$$\frac{\partial \rho}{\partial t} + \nabla \cdot (\rho \vec{v}) = 0 \tag{2}$$

$$\frac{\partial (\rho \vec{v})}{\partial t} + \nabla \cdot (\rho \vec{v} \otimes \vec{v}) = -\nabla \cdot p + \nabla \cdot \tau + \vec{S}_b + \vec{S}_p \tag{3}$$

Here, ρ, t, and p are the density, time, and pressure respectively; $\vec{v}$ is the velocity; τ is the viscous stress tensor; $\vec{S}_b$ is the body force like gravity; $\vec{S}_p$ is the source term representing the forces exerted by powders that is neglected in the one-way coupling method.

Compressibility is often ignored due to small pressure drop and low Mach number [59]. Moreover, the temperature variation of gas is quite small and out of interest so the energy equation of gas can be neglected. To describe the turbulence effects of gas flow, Reynolds-Averaging Navier-Stokes (RANS) modeling approach is generally used with the two-equation model, such as $k-\epsilon$ [60] or $k-\omega$ [61], being applied.

Powder dynamics is generally calculated through Lagrangian approach, in which drag force, inertia, and gravity are considered. Certainly, tracking each of powder particles is impossible. Discrete phase model (DPM) has been applied extensively to study the dynamics of powder stream, in which a number of powder particles with same properties are regarded as a parcel but follow the governing law of a single particle to produce statistically reasonable results (e.g., [62–64]). Thermally, laser beam and heat convection are considered for powder heating during flight. Heat transfer due to phase change was also considered by many researchers. A typical set of differential equations describing powder stream can be seen as follows,

$$\frac{d\vec{r}_p}{dt} = \vec{v}_p \tag{4}$$

$$\frac{d\vec{v}_p}{dt} = \vec{F}_{\text{Drag}} + \vec{F}_b \tag{5}$$

$$m_p c_p \frac{dT}{dt} = S_{GL} - S_{LC} - S_{LR} - S_{LP} \tag{6}$$

where r_p, m_p, c_p, and T are the position, mass, specific heat capacity, and temperature of powder; $\vec{v}_p$ is the velocity; $\vec{F}_{\text{Drag}}$ is the drag force; $\vec{F}_b$ is the body force such as gravity and buoyancy force; S_{GL} is the energy gained through laser irradiation; and S_{LC}, S_{LR}, and S_{LP} are the heat loss due to convection, radiation, and phase change during flight. The drag force, $\vec{F}_{\text{Drag}}$, is calculated through particle relaxation time [65] and models for drag coefficient such as spherical [66] and non-spherical [67] drag models. The turbulence effects on the movement of powder particles can be included, for which Stokes number (Stk) can be used as a criterion [68]. If needed, the discrete random walk model [65] is often used. The energy gained from laser irradiation and laser beam attenuation is generally computed in the same way as how the analytical models do. The convective heat term, S_{LC}, can be evaluated by the correlation relationship built by Ranz and Marshall [69, 70].

Numerical models focusing on powder stream behaviors have been developed without considering substrate effects. Lin [62] presented a numerical model for the powder stream problem in LPD, where the steady-state assumption was made for the turbulent gas flow and the standard $k-\epsilon$ turbulence model and free boundary conditions were applied. The one-way coupling technique was used to calculate the particle trajectory based on the solution of the gas flow, from which the velocity and structure of powder stream such as powder concentration could be found. Zhang et al. [71] reported a similar numerical model built in the commercial software, Fluent [72], to solve the two-phase turbulent flows based on the same physical interpretation. The impacts of nozzle geometry and shielding gas on the characteristics of powder stream were studied by introducing variations of interested parameters such as the cone angle of nozzle and the velocity of shielding gas. Bedenko et al. [73] also presented a numerical model for free powder stream considering the collisions among particles especially on the focusing areas and nozzle exit.

The movement of powder particles is influenced by powder feeders and nozzle wall due to momentum loss. A stochastic model emphasizing the particle-wall collisions with consideration of particle shape effects was developed by Pan and Liou [74] but the effects of carrier gas were considered to be negligible in the model. Later, this model was used to study the effects of the parameters of powder delivery system on the powder stream structure [75]. Pan et al. [76] also incorporated this model into the analysis of the complete two-phase powder stream from nozzles with different shapes through commercial software. Polyanskiy et al. [77] developed a numerical model to investigate the two-phase flow and applied restitution coefficient to cover the effects of nozzle wall. They found that the change of velocity of particles was not important after exiting nozzle but closely related to the wall effects.

The presence of substrate actually influences the two-phase flow field. The flow field considering the effects of substrate is quite different from previous models with free stream boundary conditions and the near-wall turbulence needs to be carefully modeled due to the impingement of gas flow. The model developed by Zekovic [78] concentrated on the fully coupled gas-powder flow with various stand-off distances for nozzles of LENS. Due to the presence of wall, near-wall turbulence modeling was also considered to take into account the viscosity-affected region near the wall. Zhu et al. [79] implemented a model through commercial software with consideration of the influences of deposited layers on the dynamics and hence distribution of powder stream, where different widths and heights of the deposited layers were applied.

Kovalev et al. [80] also solved the two-phase flow problem and considered the effects of substrate. One-way coupling strategy was applied and finite difference method (FDM) was used to calculate the flow field. The powder

particles were simulated via similar discrete Lagrangian model incorporating the particle-wall collision through the coefficient of restitution. Liu et al. [81] developed a similar model to describe the metallic powder flow based on the same idea in commercial software, where the geometry of the nozzles was modeled carefully and the influences of substrate with different surface shapes was investigated.

Thermal analysis of powder stream has been conducted by numerous models, in which laser heating is of primary importance but the heat loss by convection, phase change, and radiation is also considerable. Liu et al. [82] analyzed the heating, melting, and evaporation processes of spherical powder particle with the assumption of constant gas flow field in coaxial laser cladding. The laser intensity was assumed to be uniform across the beam and decrease with the stand-off distance. The heat convection coefficient and the total mass transfer coefficient were obtained through the built relationships involving dimensionless parameters such as Reynolds (Re), Prandtl (Pr), Nusselt (Nu), Sherwood (Sh), and Schmidt (Sc) numbers.

Wen et al. [63] developed an axisymmetrical numerical model with the two-way coupling strategy. The interaction between the laser and the powders was considered with the effective projected area of powder particles. A thermal submodel was proposed to include not only laser heating and heat loss by convection but also the latent heat during melting through the evolution of liquid fraction of the powder particles. A detailed laser profile, including convergence and divergence, shown in Fig. 4 was used, which was proven to be necessary. However, laser power attenuation was neglected.

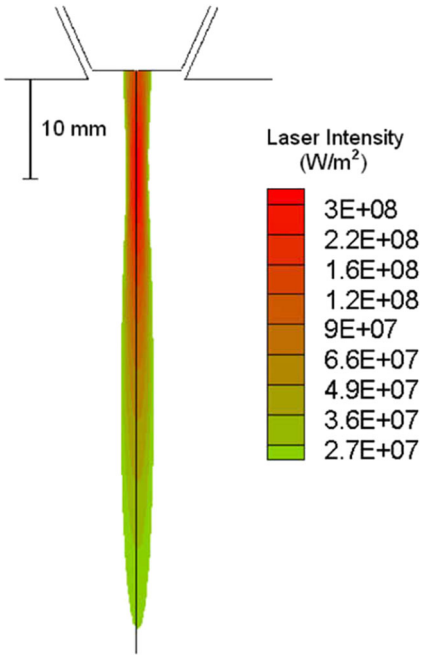

Fig. 4 Laser intensity profile (power: 300 W, radius: 0.75 mm) [63]

Ibarra-Medina and Pinkerton [83, 84] used similar numerical models to analyze the interactions among the powder stream, laser beam, and the substrate in laser cladding process. Apart from the laser irradiation, beam reflecting from substrate was also included. Efforts were put on laser attenuation due to the presence of powder cloud, in which an attenuation model similar to the one in [53] was applied. Through reverse engineering of the nozzle, Tabernero et al. [85] defined the computational domain and developed a numerical model to predict the powder flux. Later, they incorporated the attenuation model from Pinkerton [53] into their model to predict the attenuation, in which beam divergence was also included but only by modifying the power distribution [86]. Ray tracing method was used by Devesse et al. [87] to obtain the averaged laser intensity after passing through powder stream and the energy absorbed by powders. In this model, the trajectories of particles were generated by Monter Carlo technique after the calculation of gas field.

Compared with analytical model, the two-phase turbulent flow of powder stream is solved numerically based on the physical governing equations. This type of model is able to deliver physically more consistent results towards the dynamic behaviors of powder stream and hence better thermal analysis can be conducted. However, similar methods describing laser attenuation, such as the Beer-Lambert law, are also used by numerical models. Indeed, the analytical modeling method towards laser attenuation is used extensively in different kinds of modeling approach mainly because numerically solving the transport of laser beam going through powder stream is extremely complex and time-consuming.

4 Modeling of melt-pool and bulk heating

Melt-pool is central for the modeling of LPD. It accepts the heated powder stream and the laser beam after attenuation, which triggers strong transport phenomena and impacts the performance of LPD in various ways such as the shape of deposited tracks, surface quality, and microstructures. Meanwhile, bulk heating and related mechanical responses in HAZ are also greatly influenced by melt-pool due to strongly coupled heat transfer. Therefore, the modeling of melt-pool and bulk heating need to be carefully handled. Moreover, if mechanical analysis is of interest, especially the evaluation of residual stress, it can also be incorporated into the bulk thermal model as they are deeply coupled and the induced thermal strain is one of the factors causing the formation of stress.

Analytical and numerical models have been proposed for melt-pool, bulk heating, and related mechanical analysis. Like analytical models for powder stream, highly simplified assumptions are inevitable due to the complex physics related. Beside thermal profile, analytical models have been built to investigate the characteristics of geometry of melt-pool and deposited tracks. For numerical models, related conservation equations are solved through numerical methods. Note that to model the melt-pool and bulk heating in LPD, powder stream also need to be modeled as it is the starting physical process of LPD. Generally, analytical models for both powder stream and melt-pool including bulk heating are used together. Meanwhile, the numerical models for melt-pool and bulk heating have employed both analytical and numerical models for powder stream based on their specific modeling approach, which will be discussed in the remainder of this section.

4.1 Analytical models

Generally in the analytical models, conservation laws are respected but the detailed solution of liquid flow in melt-pool is neglected due to the incapability of analytical approach. Certain melt-pool behaviors such as surface tension and Marangoni effect can be reflected to enrich the physical details of analytical models. The substrate is often assumed to be semi-infinite. Note that models developed based on the experimental results and data fitting techniques (e.g., [88–90]) are not discussed in this paper.

The characteristics of melt-pool geometry and thermal profile have been investigated widely, and various models have been proposed. Labudovic et al. [91] used Green's function to solve the heat conduction equation, where the maximum surface temperature was obtained through a combination of extreme cases, i.e., laser beam stayed stationary or moved at infinite speed. Energy balance among absorbed laser energy, latent heat, and heat conducted into solid material was used to identify the boundary of the melt pool and build a steady thermal model.

Oliveira et al. [92] estimated the laser power required to melt powders and substrate based on the model from Jouvard et al. [93] and found the correlation between the geometric characteristics of the melt-pool and process parameters through experiments and analytical model. Fathi et al. [94] proposed a 3D analytical model to predict the melt pool depth, temperature distribution, and dilution. Part of the melt-pool geometry was assumed in advance with simple shape and a moving point heat source was incorporated to address the heat conduction problem and hence to obtain the phase interface as melt-pool boundary. The effects of Marangoni flow and phase change were reflected in the material properties.

The effects of surface tension were highlighted in the theoretical model by Lalas et al. [95]. At first, the deposited volume was calculated assuming that the substrate was not melted. Then, part of the substrate material and powders were assumed to be melted together. The shape of deposited layer was computed based on the assumption of circular shape for top and bottom of the deposited clad. Partes et al. [96] analytically developed a model that was able to evaluate the catchment efficiency with respect to the melt pool geometry in laser cladding. The melt pool geometry was greatly simplified as two-dimensional (2D) half circle and half ellipse. Similar assumption of the melt-pool shape was also used by many other analytical models (e.g., [97, 98]), where the limits of tracks were pre-determined as arc and/or ellipse.

A mass-energy coupled analytical model was developed by Ahsan and Pinkerton [99], which described mass addition, melt-pool, and track formation. The equation for moving Gaussian heat source from Cline and Anthony [100] was used for the melt-pool. The melt-pool was approximated by two half ellipses. Heat loss by convection and radiation were ignored while evaporation was considered. This model was solved by numerical method, where a feedback loop system was used until a stable melt-pool size was obtained.

A parametric model was presented by Wang et al. [101], where mass and energy conservation equations are represented by process parameters and melt-pool geometrical values. The width of melt-pool was assumed to be the same as its length and have a fixed ratio to its height. However, the heat loss through substrate was considered by a convective coefficient calculated through finite element method (FEM) [102]. Later, Li et al. [103] extended this model for multi-track and multi-layer situations.

The thermal profile and history have been investigated by many analytical models, in which classical solutions [104–106] towards heat conduction equation with point, line, or plane heat source have been used. Based on these classical solutions, Elsen et al. [107] presented the steady-state solutions towards point, semi-ellipsoidal, and uniform moving heat sources for semi-infinite medium, through which the impacts of the geometry of heat source were compared. Linear and surface moving heat sources were used by Pinkerton and Li [97, 108] to describe the temperature field of LPD.

Li et al. [109] proposed a thermal model by using two virtual opposite heat sources, i.e., positive and negative, to count for the effects of heat accumulation by each deposited layer. Also, reflection technique of heat source was used to generate adiabatic condition for substrate surface for both real and virtual heat sources. Similarly, superposition of the classical solutions, such as the Rosenthal's solutions [104]

of point heat source, has been used by other models with modifications to model the thermal field [103, 110, 111].

Huang et al. [112] also adopted imaginary heat sources to describe heat accumulation effects. Powder addition was regarded as a heat sink and could be combined with laser heat source. The shape of cross-section of deposited layer was assumed to be parabolic [113]. In addition to Young's equation for computing contact angle, Hoffman-Voinov-Tanner law was used to describe the spreading of liquid droplet [114]. The built model was applied in scenarios like single-track, multi-track, and multi-layer deposition.

Similar to powder stream, analytical models towards melt-pool and bulk heating also have to adopt assumptions such as pre-defined melt-pool and/or track shape, which, however, physically do not hold and can vary greatly for different process settings and parameters. In addition, the neglected transport phenomena of melt-pool greatly influences the geometrical features of fused track mainly due to capillary and thermal-capillary behaviors, which need to be carefully modeled. Nevertheless, because of the short modeling time and less work involved, analytical models towards melt-pool and bulk heating are still popular for simple estimation.

4.2 Numerical models

For numerical models targeting melt-pool, conservation equations of mass, momentum, and energy shown in Eqs. 7, 8, and 9 are generally considered,

$$\frac{\partial \rho}{\partial t} + \nabla \cdot (\rho \vec{v}) = S_m \tag{7}$$

$$\frac{\partial (\rho \vec{v})}{\partial t} + \nabla \cdot (\rho \vec{v} \otimes \vec{v}) = -\nabla \cdot p + \nabla \cdot \tau + \vec{S}_{\text{mom}} \tag{8}$$

$$\frac{\partial (\rho c_p T)}{\partial t} + \nabla \cdot (\rho c_p T \vec{v}) = \nabla \cdot (k \nabla T) + S_e \tag{9}$$

where k is heat conductivity; S_m, $\vec{S}_{\text{mom}}$, and S_e are the sources terms for mass, momentum, and energy equations; all the other variables have the same meanings as in Section 3.2 except that they are the variables for the liquid material in melt-pool. Conservation equation of species has also been added by some models. Effects of powder injection can be reflected by the source terms and calculated with the analytical or numerical models discussed in Section 3.

For bulk heating, heat conduction equation, i.e., Eq. 9 without advection term, is generally considered. As for the related mechanical analysis, residual stress evaluation is often of interest in the reviewed literature, in which elastic, plastic, and thermal strains are considered with force equilibrium. Note that the mechanical analysis in LPD deeply depends on the results of thermal calculation and that mechanical behaviors are not always analyzed in the reported models, so it will only be briefly discussed if present in the reviewed literature.

Because of the small physical scale and complex physical events of melt-pool, one type of numerical models does not explicitly model the transport phenomena in melt-pool but focuses on the bulk heating and related mechanical behaviors in part level. This type of models is called part-level model reflecting its simplification on melt-pool and concentration on bulk behaviors. The other type, melt-pool level model, computes the transport phenomena in melt-pool and bulk heating explicitly.

Note that the distinguish feature of the modeling of melt pool and bulk heating in LPD is the addition of deposited material. Since the part-level model does not include the details of melt-pool, the powder injection and the surface of melt-pool cannot be captured numerically and hence the material addition (cell addition in numerical model) needs to be set analytically. However, in melt-pool-level models, the powder injection and free surface of melt-pool can be calculated numerically without extra manual work.

4.2.1 Part-level models

For part-level models, a material deposition method needs to be applied to count for the material addition and various methods have been proposed, among which there are two widely adopted deposition methods: quiet and inactive element method [115]. In the quiet element method, or sometimes called dummy material method, the elements representing material deposition regions are present from the beginning, whose properties are manually set so that the overall results will not be affected significantly. In the inactive element method, the elements representing material deposition regions are added and connected to the existing elements at each time step. The number of elements to be added at each time step is determined by the amount of material entering melt-pool in that time step. Only active elements are considered in solution process but related boundary conditions and solver information need to be updated frequently. A typical part-level model can be seen in Fig. 5, where active and inactive mesh elements are separated by a virtual interface. Naturally thermal boundary conditions such as convection and radiation should be specified at this interface. However, this is generally neglected because the interface is hard and expensive to be captured, which may lead to inaccurate results [115].

Quiet element method Quiet element method has been used in many numerical part-level models. Wang et al. [116] developed a 3D model that employed a constant mesh to analyze the thermal field in LENS. Laser irradiation was represented by a moving point source with Gaussian distribution and applied to the top edge of the

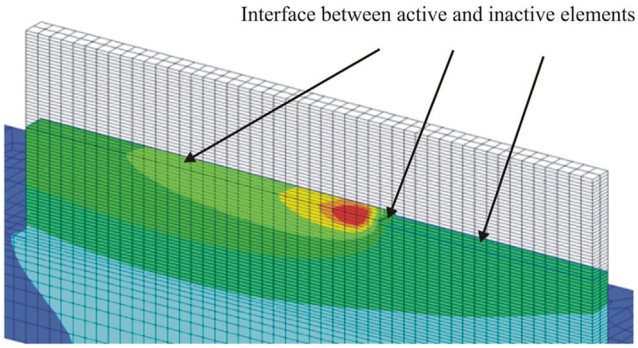

Fig. 5 Part-level model: active and inactive elements [115]

computational domain beneath the laser beam. In addition, heat convection was considered on every surface through constant convective heat transfer coefficient. Radiative heat loss was also incorporated into the model. The dummy material method was adopted and the model was built and solved by FEM in the commercial software, SYSWELD [117], to predict the temperature distribution and phase transformation in LENS. Three different types of material are considered in their dummy element method: deposited or base material, material that has not yet been deposited, and material that is being deposited. Fixed meshes are used for deposition of each layer. Through existing temperature-dependent material properties and phase diagram, they are able to take the metallurgical transformation into account. This model was also applied in many other scenarios for simulation and/or optimization [118–121].

Later, Wang et al. [122] conducted mechanical analysis based on this model. Elastic strain, strain induced by expansion or contraction of metallurgical transformation, plastic strain, and plastic strain caused by phase transformation were considered by their mechanical model built in commercial software. A model adopting similar approach was developed by Ye at al. [123] to describe the thermal behavior in LENS process but the elements to be deposited were assumed to be zero for their initial temperatures. Both 2D and 3D thermal models of LENS were presented by Yin et al. [124], where elements of deposited layer were activated together. They found that the heat transfer inside substrate was hardly captured by 2D model, which made the 3D model better from this perspective. Wang et al. [125] also developed a 2D FEM model to investigate the importance of various forms of heat transfer such as convection, conduction, and radiation, in which the thermal profile around melt-pool was calibrated by the experimental results from Hofmeister et al. [126].

A 3D thermal-mechanical model was developed by Patel and Patel [127] to estimate the thermal and mechanical behaviors of LENS process, where heat conduction and elastic, plastic, and thermal strains were considered. Another thermal-elastic-plastic model was presented by Yang et al. [128] to analyze the thermal-mechanical behavior in LENS. An element was considered active based on the criterion from Michaleris [115] if the heat source value was more than 5% of the maximum at any Gauss point in that element. An ellipsoidal volumetric heat source was used to approximate the heat input [129]. Thermal and mechanical calculation were decoupled and thermal solutions were used as input for the quasi-static mechanical analysis, where inertial effects were ignored. Elastic and perfect plastic constitutive models with the von Mises yield criterion were adopted in the model. Shah et al. [130] developed a model of the same kind and applied it to LPD process with continuous and pulsed wave laser to study the influences of powder feeding rate and laser cycle.

Thermal-mechanical analysis was also done by Chew et al. [46] for deposition in a triple-nozzle LPD process. Laser heat flux was computed excluding the energy attenuated and the energy used for powder heating. A modified conductivity factor was used to account for the transport phenomena in melt-pool [131] and Johnson-Cook model from Lee and Yeh [132] was adopted for plasticity.

Yan et al. [133] reported a 3D FEM model to obtain the thermal history and investigate the effects of cooling rate on the microstructures of deposited tracks. Residual stress prediction was incorporated into the same model and multiple laser beams of different types such as super-Gaussian, Gaussian, and inverse-Gaussian were utilized to investigate the potential combination of heat input to reduce residual stress [134]. Similar FEM thermal model was also developed by Khanafer et al. [135] with the focus on the effects of laser properties on thermal variations.

Carrier gas can impact the heat loss due to convection and hence the thermal field in the process. Pre-defined convective coefficient used in many models is not physically consistent and hence its suitability is of question. Measurement-based forced convection coefficient was included in the FEM-based numerical models by Gouge et al. [136], which was proven to be necessary. A thermal-mechanical model was developed by Heigel [137] based on the same thermal model, where the stress equilibrium equation with perfect plasticity is applied to predict the residual stress. They also showed that the convection model from experiments was necessary.

Inactive element method Inactive element method is also used widely by various numerical part-level models. Toyserkani et al. [138] developed a 3D decoupled mass-thermal model and solved it by FEM, where an effective conductivity was used to account for the melt-pool behaviors and adaptive meshing technique was applied considering the geometrical changes during deposition. They first obtained the melt-pool geometry only based on the thermal

conduction and then added the deposited material. Finally, the laser heating effects were included and the new geometry of melt-pool was calculated.

Costa et al. [139, 140] reported a thermal model to predict the temperature profile, in which phase transformation, microstructural evolution, and hardness profile were estimated through semi-empirical relations. Qian et al. [141] built a 2D FEM model to obtain the thermal history through element activation technique and to find the influences of laser properties and the sampling location of built part on thermal history and hence microstructure. Neela and De [142] developed a numerical model to describe the thermal behavior in LENS with the consideration of phase change and related latent heat. A fixed number of elements were activated each step based on the powder flow rate, capture efficiency, and scanning speed.

Mahapatra et al. [143] presented a 3D FEM model to predict the thermal profile and solidification area for pulsed-laser powder deposition through activation and deactivation technique. An average of pulsed-laser heat source for a certain amount of time was used in the model to save computational cost. Distortion and stress formation occurred in the process was investigated by Marimuthu et al. [144] through a 3D thermal-mechanical model built with inactive element method. A 2D thermal model for multi-layer deposition process was established and analyzed by Sammons et al. [145] through FEM. Temperature gradient at solidification front was first derived based on simplified conservation equations, which was added to the energy equation to take into account the solidification.

Amine et al. [146] implemented a 3D thermal model and applied the inactive element method to simulate the building process of thin-wall structure. Through this type of model, the impact of process parameters such as laser power and scanning speed on the characteristics of built parts such as remelted height and cooling was investigated [147]. Similar models were also implemented by Hochmann and Salehinia [148] to study the effects of heat convection coefficient of substrate on the thermal profile and history. Walker et al. [149] adopted the analytical model developed by Ahsan and Pinkerton [99] and proposed a thermal-mechanical model to predict the residual stress. The track profile was calculated by the analytical model and fed into a FEM model for thermal and mechanical analysis.

Other methods Beside the aforementioned two popular strategies for material addition, models with other ideas towards material deposition have been developed. A numerical model with a new material deposition method, i.e., hybrid element method, was proposed by [115], which combined the features of both quiet element and inactive element approaches. Elements were initially set to be inactive and then they were switched to quiet on a layer-by-layer manner to accelerate computation. Based on this hybrid approach, models incorporating the mechanical analysis to predict the residual stress through stress equilibrium equation were proposed [150, 151].

Peyre et al. [152] reported a two-step model to estimate the shape of built tracks and to simulate thermal behaviors during the process through commercial software. First, the geometry of walls was determined by a hybrid approach, in which the 3D fusion isotherm plane was computed numerically and then fitted to a 3D ellipse. Mass and energy balances were used to calculate the layer height and an iterative method was used to calculate the width of layer. Then, FEM was used to solve the heat transfer accompanying the deposition process with the obtained geometry of deposited tracks in the first step. Kumar et al. [153] proposed a 2D model based on a modified heat conduction equation, where the reference frame in this model was built with respect to the moving laser beam and hence a constant moving velocity was added in the advection term in energy equation. The impacts of heated powders and latent heat were both covered by source terms and the free surface of melt-pool was described by a force balancing equation. FVM method was employed to solve the model.

Hofman et al. [154] proposed a new method that solved an additional partial differential equation (PDE) beside the common heat conduction equation for clad surface based on energy conservation. To save computational cost due to potential remeshing and the large number of elements, both of these PDEs were transformed to the specified computational domain and solved simultaneously [155]. Birnbaum et al. [156] developed a 3D transient thermal model in commercial software based on the Arbitrary Lagrangian-Eulerian (ALE) method [157] to account for the mass addition, which was incorporated by mesh deformation. Thermal analysis was conducted, in which the effects of phase transformation and latent heat were incorporated into the heat capacity. Bedenko et al. [158] used a surface equation based on kinematic compatibility and the distribution of powder mass flow [159] to describe the surface changes during process. The calculated heat content of the injected particles and evaporation were all included in the boundary condition of heat conduction that was solved by FDM with immersed boundary method and ghost nodes [160].

From the above discussion, it can be found that to count for the material addition in part-level models, various methods have been proposed such as the quiet and inactive element methods. The difference between these two popular approaches is that the quiet element method assumes the elements (or cells) representing the material to be deposited are present from the beginning while in inactive element method only active elements are considered. Apart from

these two methods, the hybrid method dealing with the material deposition developed by Michaleris [115] has also been used in many models. The shape of melt-pool and deposited tracks have been considered by many part-level models, in which various methods, such as ALE or relations derived from conservation or balancing equations, have been applied to describe the surface of melt-pool and deposited tracks and hence to enrich the physical details of part-level models.

4.2.2 Melt-pool Level

The part-level models discussed above simplify the transport phenomena in melt-pool, which, however, have significant impacts on the whole deposition process. More sophisticated models have been proposed to take into account the transport phenomena in melt-pool, which also enables the possibility to truly couple the powder stream and melt pool in LPD. Models numerically describing both powder stream and melt-pool and coupling them together have been presented. However, because of high computational cost involved, fully coupled numerical approach has not been extensively applied. Instead, many models apply the hybrid approach, i.e., numerical model for melt-pool and analytical model for powder stream. Generally, major physical events considered for melt-pool in the reviewed literature are heat transfer, phase change, powder injection, fluid dynamics, wetting behaviors, and Marangoni effect. To count for the mushy zone around solid-liquid interface, the continuum model from Bennon and Incropera [161, 162] is extensively applied, where the mushy zone is assumed to be porous. Boussinesq approximation is also adopted by many researchers to cover the effects of natural convection in melt-pool. The focus of this subsection will be put on the modeling of melt-pool as the modeling of bulk heating in HAZ is the same as the part-level models discussed in Section 4.2.1, in which heat conduction dominates.

Models in hybrid approach Melt-pool-level model allows for the true coupling between the powder stream and melt-pool processes and various hybrid models have been presented. To describe the free surface of melt-pool, level-set method [163, 164] has been widely adopted. Han et al. [33] developed a 2D hybrid continuum model, in which the level-set method was used not only for free surface evolution but also the mass addition due to powder injection. The injecting powder particles were treated as droplet and hence can be implicitly calculated by the level-set method as shown in Fig. 6. The evaporation of material was also included. Mushy zone was approximated as porous media and the continuum model from Bennon and Incropera [161, 162] was applied. Averaged physical properties and Darcy's law with Kozeny-Carman equation for permeability were used, which were also extensively adopted by the models of this type. The built numerical model was solved by FDM. This type of model was also applied in other scenarios such as laser material processing, cladding, and repairing to analyze the behaviors of melt-pool [165–167].

Using the similar modeling strategy towards melt-pool, Qi et al. [54] developed a model to simulate the melt-pool, in which the impact force caused by powder particles were neglected and only the mass and energy addition were considered and incorporated into the level-set equation. This model was modified by He and Mazumder [55] and He et al. [168] through adding the evolution of solute concentration, where the boundary condition at the solidification interface was given as a Robin condition of the solute concentration. Liu and Qi [56] developed a similar model for melt-pool, where a smoothing function was used at the phase interface with a fixed transition thickness to smooth the physical properties. Later, the powder mass concentration from Pinkerton and Li [44] was applied instead of simplified Gaussian distribution to consider the effects of the cone angle of nozzle and hence the convergence of powder stream on the laser powder interaction [57]. Lee et al. [169] incorporated the effects of vaporization processes into the mass and energy equations as a volume source in a similar model to study the effects of laser distribution on the transport phenomena of melt-pool. Li et al. [170] also presented a similar model to compare the deposition processes with lasers of pulsed and continuous wave modes.

Apart from the level-set method, other methods dealing with free surface evolution have been applied such as the ALE method and the volume of fluid (VOF) method [171]. Morville et al. [172] developed a 2D FEM model through commercial software to study the impacts of various process parameters on surface finish of LPD. The ALE method was employed to capture the surface evolution of melt-pool and a sink term representing the thermal influences of the neglected third dimension was applied in energy equation to suit experimental settings. The ALE method was also used to track the liquid/gas interface by Gan et al. [173] and in addition to flow velocity, a Gaussian velocity distribution was applied to represent the effects of mass addition. Song et al. [174] developed a melt-pool level model in commercial software based on the analytical powder stream model from Chew et al. [46] for triple-nozzle LPD system. The incident direction of laser beam to melt-pool surface was considered and the ALE method was used only on the melt-pool surface to capture the free surface evolution.

Lee et al. [175] developed a transport model using the VOF method to track the surface in laser cladding. Source terms were used in conservation equations to represent the effects of injected powders but the effects of the mushy zone were not included. Surface-active elements were considered

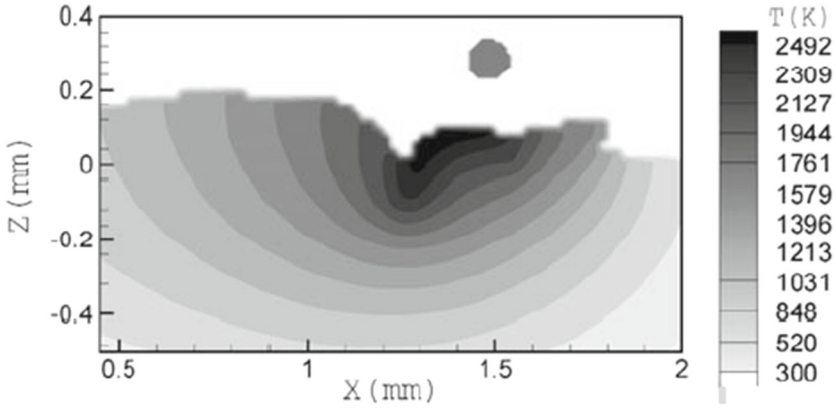

Fig. 6 Modeled melt-pool profile, temperature distribution, and powder injection [165]

when modeling Marangoni effect. Resulted flow pattern in melt-pool was shown in Fig. 7, from which it could be found that the Marangoni effect and hence the relationship between surface tension and temperature have an important impact on the flow pattern and hence the morphology of melt-pool. Lee et al. [176] used this model to investigate the effects of the thermo-capillary gradient on melt-pool behaviors. Lee and Farson [177] applied this model to simulate the multi-layer single-track deposition. In the model developed by Dubrov et al. [178], a hybrid level-set and VOF method was used to track the free surface. The impact of momentum of powder stream was included in the evolution equation of volume fraction.

Assumptions for melt-pool such as flat surface have also been employed by some models. Vasquez et al. [179] presented a quasi-stationary melt-pool level FEM model for LPD through commercial software, where the cross-section of melt-pool was assumed to be semi-circular and the escaping vapor was calculated based on Stefan's condition [180]. Manvatkar et al. [181, 182] developed a 3D transient model to predict the temperature, velocity, and melt-pool geometry profiles. The melt-pool free surface was assumed to be flat and mesh evolution was similar to the inactive element method introduced in Section 4.2.1, where the cells to be deposited were assigned properties of protecting gas and switched to the properties deposited material if laser beam was upon them. Energy absorption and laser attenuation were taken into account by a source term. Later, mechanical analysis was incorporated into a similar model to estimate the residual stress and distortion based on the obtained thermal results [183, 184].

Models in numerical approach Instead of using analytical model of powder stream, models have also been developed to fully couple powder stream and melt-pool numerically. A comprehensive numerical model was developed by Wen and Shin [185] for melt-pool with a modified level-set equation to describe the free surface of melt-pool. The impact of powder injection on free surface was added into the speed term in level-set equation and after transformation, a conservative form of level-set function was derived and could be solved in an implicit way with other governing equations. Gas-powder two-phase turbulent flow was solved numerically and coupled with melt-pool models by providing the obtained powder mass concentration to obtain the growth velocity of free surface. Continuum models from Bennon and Incropera [161, 162] were applied not only to deal with mush-zone but also the interface between

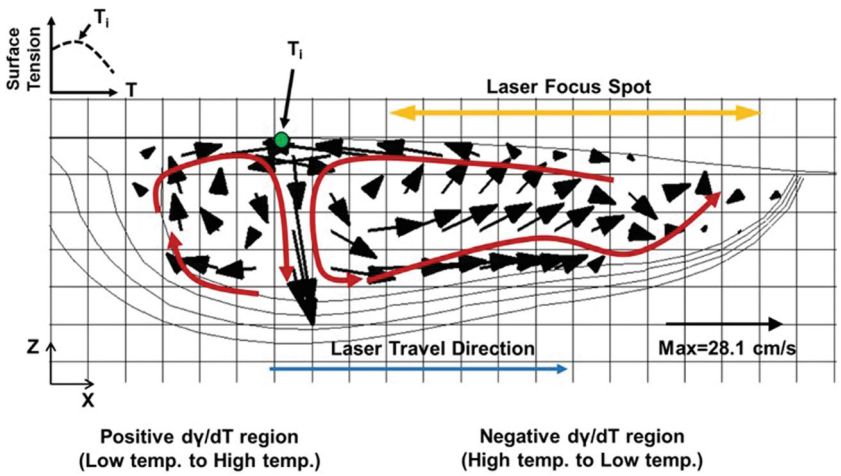

Fig. 7 Flow pattern in melt-pool [175]

gas and metal. Turbulence effects were included based on the effective thermal conductivity [186] and instead of using effective viscosity, an equivalent surface tension coefficient was adopted to ensure the numerical stability and meanwhile to keep the extent of the Marangoni flow and the ratio of advection to conduction [187]. This model was also used in other scenarios such as multi-track and off-axis deposition [188–190].

Katinas et al. [191] added the feature of powder capture into this model by only allowing powders injecting into the area of melt-pool free surface above liquidus temperature. The powders were added only if both the injected powders and the corresponding melt-pool regions remained liquid after heat transfer happened [59]. Ibarra-Medina et al. [32] reported a similar fully numerical model solved by commercial software except using VOF method to track the free surface.

Through the above discussion, it can be seen that dynamically, the capillary and thermo-capillary behaviors of liquid material are of great importance towards the transport process and the profile of melt-pool. Mushy zone has been considered by many melt-pool level models through the continuum model developed by Bennon and Incropera [161, 162]. Different methods have been applied to deal with the free surface of melt-pool, which can also incorporate powder injection to fulfill the coupling between powder stream and melt-pool. Numerical melt-pool models coupled with numerical powder stream model are physically more complete but require more modeling work and computational power, which makes the hybrid modeling approach popular.

5 Discussion

5.1 Modeling approaches for LPD

The inherent physical process of LPD consists of strongly coupled physical phenomena, which makes its modeling rather complex. As it can be seen from the discussion above, there are in general three approaches towards the overall modeling of LPD, i.e., analytical, numerical, and hybrid approaches, which are summarized in Table 1 together with frequently used modeling methods and assumptions from the reviewed literature for related physical processes, i.e., powder stream, melt-pool, and bulk heating. These modeling approaches and methods will be detailedly discussed in the remainder of this section.

Due to the complexity of LPD process, analytical approach needs to use highly simplified assumptions and hence greatly limits its physical consistency and accuracy. The primary focus of analytical models towards powder stream is the dynamics and structure of powder stream such as the distribution of powder concentration, which also enables the related thermal analysis and have been used widely by models in hybrid approach. For melt-pool and bulk heating, analytical models have been mainly used to predict the dimensions of melt-pool and the thermal profile of built part.

Meanwhile, numerical modeling approach has become more and more popular especially with the development of computational resources. The conservation laws of mass, momentum, energy, and possibly species are followed to build the numerical models, which then can be solve by computational techniques. Due to specific research interests and high computational cost, some of the numerical models neglect the transport phenomena of melt-pool and only focus on the bulk thermal behaviors and induced thermal strains if of interest. Nevertheless, many numerical models start to count for the transport behaviors in melt-pool for better physical consistency and more accurate prediction of thermal profile and shape of deposited tracks. The results from the modeling of melt-pool also plays a crucial role as input for subsequent microstructural modeling.

However, fully coupled numerical models of powder stream and melt-pool is not computationally trivial, and hence, many models from the reviewed literature have adopted the hybrid approach as a compromising approach, which uses an analytical model for powder stream and then couples it with subsequent numerical models for melt-pool and bulk heating.

5.1.1 Modeling for powder stream and laser heating

Both analytical and numerical models for powder stream have been developed, some of which also consider its heating effects due to laser beam and the attenuation of laser beam going through powder stream. Due to the huge number of injected particles in LPD, it is almost impossible to capture the trajectory of each particle even though the volume fraction of powders is quite low. Also, due to the presence of two-phase turbulent flow and laser beam interaction, modeling assumptions are inevitable and both analytical and numerical models have been developed.

Powder concentration is usually a primary goal for analytical models that can potentially be used with subsequent melt-pool and bulk heating models. Gaussian-type analytical models have been used extensively, in which the distribution of powder concentration is assumed to be Gaussian. However, some details of powder stream are still unavailable, such as the boundaries of powder stream, and need to be assumed manually. For example, the convergence and divergence angles of powder stream used in analytical models need to be assumed so that the powder concentration can be computed based on the assumed Gaussian formulation. More importantly, the Gaussian distribution is

Table 1 Modeling methods and assumptions for physical processes in LPD

Physical process / Modeling approach	Powder stream	Melt-pool	Bulk heating
Analytical	Shape and dynamic profile: Gaussian concentration; assumed boundaries, velocities Thermal analysis: iterative model or assumed temperature profile; Laser attenuation: Mie's theory, Beer-Lamber law or neglected	Shape profile: pre-determined shapes or neglected Thermal analysis: details neglected; solved with bulk heating or assumed temperature profile	Thermal analysis: classical solutions (e.g., Rosenthal's solutions); superposition; virtual sources
Hybrid	Same as above	Same as below (melt-pool level) or above (part level)	Same as below
Numerical	Shape and dynamic profile: two-phase turbulent flow model Thermal analysis: energy conservation equation; Laser attenuation: Mie's theory; Beer-Lamber law; neglected	Shape profile: computed from temperature field Thermal analysis: detailed description by solving conservation equations (mass, momentum, energy)	Thermal analysis: heat conduction

not universal. Although the Gaussian distribution has been experimentally validated in free powder stream but the substrate or deposited layers in LPD process can deeply impact its distribution.

Unlike analytical models, numerical models apply computational techniques to solve the governing equations of the two-phase flow and fewer assumptions are adopted, which are expected to produce physically more consistent results. The concentration of powder can be calculated based on the resulted trajectories of powder parcels in DPM, which has been used widely in the modeling of powder dynamics. The continuum and discrete models are applied to gas and powder phases respectively and then coupled together through one-way or two-way coupling strategy. Such models have been embedded in many commercial CFD softwares like Fluent, CFX [192], and FLOW-3D [193].

To compute the thermal profile of powder stream, especially the heating effects due to laser beam, the concentration profile or the dynamic behavior of powder stream needs to be known in advance through assumptions or computed results in either analytical or numerical models. The concentration profile or the location of powders in analytical or numerical models determines the energy absorbed from laser beam due to the spatial distribution of laser intensity (e.g., Gaussian). Conservation of energy is considered in most models to compute the thermal profile of powder stream, which generally needs to be solved through iterative techniques, even in the analytical models discussed in Section 3.

The most important heating source for powders is laser beam, which requires careful modeling due to the attenuation effects of powder stream. Models based on Mie's theory and Beer-Lambert law have been developed and used while models without considering attenuation of laser beam have also been proposed and applied. Clearly, including the attenuation effects is not only physically more consistent but also benefits the successive modeling as the laser beam after attenuation irradiates the surface of melt-pool, substrate, or deposited layers.

5.1.2 Modeling for melt-pool and bulk heating

Melt-pool connects powder stream and deposited material. Its dynamical and thermal behaviors dictate the phase change, i.e., melting and solidification, in LPD and hence the properties of built parts such as the porosity and morphology. Similar to the models built for powder stream, analytical and numerical models have been developed with certain assumptions, in which conservation laws are respected in both approaches while the governing equations are developed and solved differently.

Analytical models generally adopt aggressive assumptions, especially towards melt-pool, and available solutions from classic problems. Rosenthal's solutions to heat

conduction problems in semi-infinite domain are used extensively in the thermal modeling, which, however, cannot count for the complex build process of LPD such as multi-layer deposition and repetitive scanning in LPD. Improvements have been made for such scenarios such as the superposition of solutions and the virtual heat sources to cover the heat accumulation effects.

Melt-pool profile has also been investigated through analytical approach but due to the complex physics involved, the geometrical profile generally needs to be set manually in advance for analytical models, such as the half circle and half ellipse in 2D situation. Pre-determined shape of melt-pool provides great ease in modeling melt-pool, which, however, is by no means consistent with the real physics especially in complex cases such as multi-layer building process.

Numerical models developed towards melt-pool and bulk heating solve the governing equations directly through various computational techniques such as FEM, FVM, etc. There are two type of models dealing with different scales, i.e., part level and melt-pool, because of different research interests, modeling complexity and computational cost. The former concentrates on the heating behaviors of entire part and simplifies the transport phenomena of melt-pool. Only the heat conduction equation needs to be solved (apart from potential mechanical analysis), and the related computational cost is not high due to relatively large element size. The latter explicitly calculates the physical events of melt-pool and couples it with the heat conduction model of HAZ, which naturally requires more modeling work such as meshing especially near the melt-pool region. The computational cost is also higher since the element size needs to be very small to capture the behaviors of melt-pool.

Numerical part-level models generally solve the heat conduction equation and some of them use certain modifications to represent the impacts of melt-pool, such as modified heat conductivity. An important feature of part-level models lies in the modeling of material addition. Because there is no explicit modeling of the melt-pool, assumptions of adding material have to be made such as the amount of material to be added at each time step. Two popular methods have been proposed and used widely, i.e., quiet element method and inactive element method.

The quiet element method considers the material elements, including the elements to be deposited, to be present from the starting time while the inactive element method activates the elements as they are deposited. Because of the scaling technique used in the quiet element method to minimize the impacts of virtual elements, ill-conditioned problems may occur for solution process. But since the elements are present from the starting point, repeated solver initialization and updates are not needed. On the contrary, due to the addition of new elements in inactive element method, the solver needs to be updated and initialized repeatably but a smaller algebraic system can be obtained because only active elements are considered. A hybrid method trying to combine the advantages of both methods has also been proposed, in which elements are activated layer by layer but in each layer, quiet elements are used [115].

Numerical part-level models neglect the transport events in melt-pool, which impacts not only the thermal field of melt-pool and HAZ but also the coupling between the powder stream and melt-pool. The addition of material in part-level models is generally simplified as elements addition without considering the geometrical features of the melt-pool and deposited tracks. With melt-pool level models, the material addition can be calculated without aforementioned rough assumptions. Mass, momentum, and energy carried by powder stream can be extracted and used in melt-pool computation.

To count for the mushy zone near the interface between solid and liquid phase, models with averaged formulation from Bennon and Incropera [161, 162] have been developed, in which averaged variables and properties are computed through mass and volume fraction. The turbulence effects in melt-pool have been considered by some models with simplification but the explicit modeling of turbulence is rare possibly due to high computational cost.

The modeling of free surface of melt-pool is of great importance as it accepts the injected powders and the attenuated laser beam and impacts the morphology of deposited tracks. It has been modeled through various methods, in which level-set, VOF and ALE methods have been widely used. Level-set method uses an additional transport PDE to describe the newly defined level-set variable, in which 0, positive and negative values represent the cell on, inside and outside free surface. A transport term with local velocity and the terms representing mass addition and/or the forces acting on the free surface can be used to model the evolution of free surface. With level-set method, the normal and curvature of the free surface can be easily computed through the level-set variable, which then simplifies the calculation of capillary and thermal-capillary forces. However, mass conservation is problematic for level-set method. This method has been used widely in modeling melt-pool of LPD as discussed in Section 4.

VOF also employs an addition PDE to calculate the volume fraction of fluid in each cell. However, the interface of each cell needs to be reconstructed based on the volume fraction in neighbor cells and then the surface normal and curvature can be calculated, which is more complex than level-set method. Mass is conserved through VOF method

but the computed free surface tends to be smearing. Details of level-set and VOF methods can be seen in Maitre [194] and Gibou et al. [195].

ALE uses a completely different methodology to deal with free surface, in which nodes of mesh can move in an arbitrary way and hence to cover the movement of free surface. However, the cost of remeshing is not trivial. With ALE, the formulation of governing equations needs to be modified to incorporate the effects of mesh moving, in which the meshing moving velocity need to be included into the advection terms. A Lagrangian boundary condition with zero normal velocity can be directly imposed on the free surface. Details of ALE can be found in Donea et al. [196].

5.2 Physical aspects for the modeling of LPD

For the modeling of LPD, the following physical aspects are essential and need to be carefully treated. First and foremost, the physical properties of used material, such as density, specific heat, surface tension and its temperature coefficient, thermal conductivity, and viscosity as well as their relationships with physical variables such as temperature, are of primary importance. As the input conditions used in every stage of modeling, their accuracy is crucial for the performance of developed models especially for the detailed physical description of LPD. For example, as shown in Fig. 7, the temperature-dependent surface tension and its gradient can substantially impact flow patterns and hence the shape of melt-pool and deposited tracks. Apart from temperature, surface tension can also be dependent on certain element concentration for alloy material.

Also, attention needs to be put on the powder stream and its interaction with laser beam as they deeply affect the spatiotemporal distribution of mass, momentum, and thermal profile of the injecting powders, which then impacts the melt-pool and the whole process. Attenuation of laser beam due to powder stream should be considered and calculated as the laser beam after attenuation directly irradiates the surface of melt-pool and contributes greatly to the heat transfer and thermal-driven flow of melt-pool. In addition, laser beam is assumed by many models to be collimated, which is generally not the case as it also involves convergence and divergence. Because the intensity of laser beam in LPD is generally very large, such simple simplification of laser profile can produce quite inaccurate laser intensity and hence errors of the whole modeling of powder stream. The detailed profile of laser beam needs to be considered because of the large value of laser intensity. For example, in Gaussian beam, depth of field (DOF), half angle, and beam radius need to be applied to build a relatively complete laser profile.

Furthermore, melt-pool is considered as the central part of modeling for LPD as it connects the powder feeding and bulk heating. Melt-pool accepts the injected powder particles, which contribute to the formation of deposited tracks after going through phase changes. However, not all of the powder particles are generally captured by the melt pool and hence the catchment efficiency need to be carefully considered to determine how many powder particles are actually used to build the deposited part. The mass, momentum, and energy carried by the captured powder particles can be influential on the thermal and dynamic profiles of melt-pool. The addition of mass and energy from the captured powder particles are generally counted when modeling the interaction of powder stream and melt-pool in the reviewed literature. The most considered phenomena from the reviewed literature also include liquid flow dynamics, wetting behavior, Marangoni effect, heat transfer, and phase transformation (evaporation, melting, and solidification), among which Marangoni effect deeply affects the flow pattern and the shape of melt-pool.

Due to substantial heat transfer and repeated scanning, residual stress can be formed and even distortion can occur, which can potentially change the building conditions of LPD such as the geometry of the built parts. Although the mechanical analysis was not discussed in detail in this paper, it can be added to the thermal models without much difficulty provided that the thermal model is valid. The real difficulty in modeling LPD lies in the modeling for material addition and heat transfer due to laser beam.

5.3 Suggestions for the future modeling of LPD

For the future modeling of LPD, several suggestions are made as follows. First, for different research focus, both effectiveness and cost of the model need to be considered. The fully numerical model should be considered for detailed description and prediction of LPD. Actually, the complete modeling work of LPD process also consists of the evolution of microstructures and properties, which can further complete the physical details and enable the valuable coupling between macroscopic and microscopic models. Naturally, the work load and computational cost of such complete models are extremely high. Beside aforementioned complex models, relatively simple models can also be useful and satisfactory for many research purposes. For example, the part-level models for melt pool and bulk heating are very popular in predicting bulk thermal and mechanical behaviors even though the transport phenomena are simplified. Also, the analytical models of powder stream have been widely used in the models adopting hybrid approach and proved to be valid.

Furthermore, so far, the majority of the reviewed models have focused on simple geometries such as single track, multi-track, and multi-layer since the computational cost is relatively low compared with full-scale LPD

simulation. Currently limitations from computational aspect and modeling approach are making it difficult to model all of the physical phenomena in LPD with high fidelity. Based on existing resources, compromises have to be made between the speed and accuracy. Numerical models can take advantage of the high-performance computing resources if available.

Meanwhile creative modeling approaches or numerical procedures should also be developed. The hybrid approach discussed before is a feasible choice for those who do not access to high-end computing resources. It may also be feasible and better to numerically calculate the powder stream in a steady-state way and export the results of powder stream, such as the flux profile of mass, momentum, and energy of powder stream, into the successive melt-pool model to obtain physically more consistent and accurate results. It should also be noted that since there are a large number of process parameters involved in LPD process, including many uncertain parameters whose effects have not been fully understood. Therefore, uncertainty quantification can be conducted to increase the performance of built models.

Finally, it is worthwhile to note that the techniques from machine learning (ML) [197] have been used in some other AM processes to work with simulation models for predictions and optimization [198, 199]. Potential collaboration with ML models for LPD may also be beneficial. For instance, through ML models built on the results obtained from physic-based model (or experiment) and process parameters, preliminary optimization can be conducted. Then, further optimization can be conducted based on modeling (or experiments) to choose optimal parameters from the resultant optimized space to accelerate optimization.

6 Conclusions

In this paper, a thorough review has been given towards the modeling work of LPD process with the focus on the powder stream, melt-pool, and bulk heating. Different modeling approaches, i.e., analytical, numerical, and hybrid, have been summarized and compared. Reported models found in the reviewed literature have been discussed in detail for different physical process of LPD. Various modeling strategies dealing with laser powder interaction, material addition, and the coupling between powder stream and melt pool have also been carefully reviewed. Considerations and suggestions for the modeling of LPD have been given at last.

Funding information This research was supported by the Natural Sciences and Engineering Research Council of Canada (NSERC) Collaborative Research and Development Grant, CRDPJ 479630. The lead author also receives partial funding from NSERC Collaborative Research and Training Experience Program Grant, CREATE 449343. The author would also like to thank the McGill Engineering Doctoral Award (MEDA).

References

1. Gao W, Zhang Y, Ramanujan D, Ramani K, Chen Y, Williams CB, Wang CC, Shin YC, Zhang S, Zavattieri PD (2015) The status, challenges, and future of additive manufacturing in engineering. Comput Aided Des 69:65–89. https://doi.org/10.1016/j.cad.2015.04.001
2. Ngo TD, Kashani A, Imbalzano G, Nguyen KT, Hui D (2018) Additive manufacturing (3D printing): a review of materials, methods, applications and challenges. Compos Part B Eng 143:172–196. https://doi.org/10.1016/j.compositesb.2018.02.012
3. ISO/ASTM52900-15 (2015) Standard terminology for additive manufacturing technologies - general principles - terminology. ASTM International, West Conshohocken
4. Frazier WE (2014) Metal additive manufacturing: a review. J Mater Eng Perform 23:1917–1928. https://doi.org/10.1007/s11665-014-0958-z
5. Herzog D, Seyda V, Wycisk E, Emmelmann C (2016) Additive manufacturing of metals. Acta Mater 117:371–392. https://doi.org/10.1016/j.actamat.2016.07.019
6. DebRoy T, Wei HL, Zuback JS, Mukherjee T, Elmer JW, Milewski JO, Beese AM, Wilson-Heid A, De A, Zhang W (2018) Additive manufacturing of metallic components – process, structure and properties. Prog Mater Sci 92:112–224. https://doi.org/10.1016/j.pmatsci.2017.10.001
7. Lee H, Lim CHJ, Low MJ, Tham N, Murukeshan VM, Kim YJ (2017) Lasers in additive manufacturing: a review. Int J Precis Eng Manuf-Green Technol 4:307–322. https://doi.org/10.1007/s40684-017-0037-7
8. Taminger K, Hafley R (2003) Electron beam freeform fabrication: a rapid metal deposition process. Proceedings of the 3rd Annual Automotive Composites Conference
9. Stecker S, Lachenberg K, Wang H, Salo R (2006) Advanced electron beam free form fabrication methods & technology. Amer Weld Soc Conf 17:35–46
10. Kakinuma Y, Mori M, Oda Y, Mori T, Kashihara M, Hansel A, Fujishima M (2016) Influence of metal powder characteristics on product quality with directed energy deposition of Inconel 625. CIRP Ann 65:209–212. https://doi.org/10.1016/j.cirp.2016.04.058
11. Heralić A, Christiansson AK, Lennartson B (2012) Height control of laser metal-wire deposition based on iterative learning control and 3D scanning. Opt Lasers Eng 50:1230–1241. https://doi.org/10.1016/j.optlaseng.2012.03.016
12. Syed WUH, Pinkerton AJ, Li L (2005) A comparative study of wire feeding and powder feeding in direct diode laser deposition for rapid prototyping. Appl Surf Sci 247:268–276. https://doi.org/10.1016/j.apsusc.2005.01.138
13. Syed WUH, Pinkerton AJ, Li L (2006) Combining wire and coaxial powder feeding in laser direct metal deposition for rapid prototyping. Appl Surf Sci 252:4803–4808. https://doi.org/10.1016/j.apsusc.2005.08.118
14. Costa L, Vilar R (2009) Laser powder deposition. Rapid Prototyp J 15:264–279. https://doi.org/10.1108/13552540910979785
15. Collins PC, Banerjee R, Banerjee S, Fraser HL (2003) Laser deposition of compositionally graded titanium-vanadium and titanium-molybdenum alloys. Mater Sci Eng A 352:118–128. https://doi.org/10.1016/s0921-5093(02)00909-7

16. Wu D, Liang X, Li Q, Jiang L (2010) Laser rapid manufacturing of stainless steel 316l/Inconel718 functionally graded materials: microstructure evolution and mechanical properties. Int J Opt 2010:1–5. https://doi.org/10.1155/2010/802385
17. Reichardt A, Dillon RP, Borgonia JP, Shapiro AA, McEnerney BW, Momose T, Hosemann P (2016) Development and characterization of Ti-6Al-4V to 304l stainless steel gradient components fabricated with laser deposition additive manufacturing. Mater Des 104:404–413. https://doi.org/10.1016/j.matdes.2016.05.016
18. Korinko P, Adams T, Malene S, Gill D, Smugeresky J (2011) Laser engineered net shaping® for repair and hydrogen compatibility. Weld J 90:171–181
19. Fang J, Dong S, Li S, Wang Y, Xu B, Li J, Liu B, Jiang Y (2019) Direct laser deposition as repair technology for a low transformation temperature alloy: microstructure, residual stress, and properties. Mater Sci Eng A 748:119–127. https://doi.org/10.1016/j.msea.2019.01.072
20. Zhang X, Pan T, Li W, Liou F (2019) Experimental characterization of a direct metal deposited cobalt-based alloy on tool steel for component repair. JOM 71:946–955. https://doi.org/10.1007/s11837-018-3221-5
21. Hy Zhao, Ht Zhang, Xu Ch, Xq Yang (2009) Temperature and stress fields of multi-track laser cladding. Trans Nonferrous Metals Soc China 19:s495–s501. https://doi.org/10.1016/s1003-6326(10)60096-9
22. Scheitler C, Hugger F, Hofmann K, Hentschel O, Baetzler T, Roth S, Schmidt M (2016) Experimental investigation of direct diamond laser cladding in combination with high speed camera based process monitoring. J Laser Appl 28:022304. https://doi.org/10.2351/1.4944004
23. Griffith M, Keicher D, Atwood C, Romero J, Smugeresky J, Harwell L, Greene D (1996) Free form fabrication of metallic components using laser engineered net shaping (LENS™). Proceedings of the Solid Freeform Fabrication Symposium, pp 125–131
24. Thompson SM, Bian L, Shamsaei N, Yadollahi A (2015) An overview of direct laser deposition for additive manufacturing; part i: transport phenomena, modeling and diagnostics. Add Manuf 8:36–62. https://doi.org/10.1016/j.addma.2015.07.001
25. Shamsaei N, Yadollahi A, Bian L, Thompson SM (2015) An overview of direct laser deposition for additive manufacturing; part ii: mechanical behavior, process parameter optimization and control. Add Manuf 8:12–35. https://doi.org/10.1016/j.addma.2015.07.002
26. Griffith M, Schlienger M, Harwell L, Oliver M, Baldwin M, Ensz M, Nelson D (1998) Thermal behavior in the LENS process. Proceedings of the Solid Freeform Fabrication Symposium
27. Kahlen FJ, Kar A (2001) Tensile strengths for laser-fabricated parts and similarity parameters for rapid manufacturing. J Manuf Sci Eng 123:38–44. https://doi.org/10.1115/1.1286472
28. Pinkerton AJ (2015) Advances in the modeling of laser direct metal deposition. J Laser Appl 27:S15001. https://doi.org/10.2351/1.4815992
29. Martukanitz R, Michaleris P, Palmer T, DebRoy T, Liu ZK, Otis R, Heo TW, Chen LQ (2014) Toward an integrated computational system for describing the additive manufacturing process for metallic materials. Add Manuf 1-4:52–63. https://doi.org/10.1016/j.addma.2014.09.002
30. Francois M, Sun A, King W, Henson N, Tourret D, Bronkhorst C, Carlson N, Newman C, Haut T, Bakosi J, Gibbs J, Livescu V, Wiel SV, Clarke A, Schraad M, Blacker T, Lim H, Rodgers T, Owen S, Abdeljawad F, Madison J, Anderson A, Fattebert JL, Ferencz R, Hodge N, Khairallah S, Walton O (2017) Modeling of additive manufacturing processes for metals: challenges and opportunities. Curr Opin Solid State Mater Sci 21:198–206. https://doi.org/10.1016/j.cossms.2016.12.001
31. Picasso M, Marsden CF, Wagniere JD, Frenk A, Rappaz M (1994) A simple but realistic model for laser cladding. Metall and Mater Trans B 25:281–291. https://doi.org/10.1007/bf02665211
32. Ibarra-Medina J, Vogel M, Pinkerton AJ (2011) A cfd model of laser cladding: from deposition head to melt pool dynamics. Proceedings ICALEO'2011, pp 23–27
33. Han L, Phatak KM, Liou FW (2004) Modeling of laser cladding with powder injection. Metall and Mater Trans B 35:1139–1150. https://doi.org/10.1007/s11663-004-0070-0
34. Huang YL, Liu J, Ma NH, Li JG (2006) Three-dimensional analytical model on laser-powder interaction during laser cladding. J Laser Appl 18:42–46. https://doi.org/10.2351/1.2164476
35. Vesilind P (1980) The rosin-rammler particle size distribution. Resour Recover Conserv 5:275–277. https://doi.org/10.1016/0304-3967(80)90007-4
36. Xie J, Kar A, Rothenflue JA, Latham WP (1997) Temperature-dependent absorptivity and cutting capability of co2, nd:yag and chemical oxygen–iodine lasers. J Laser Appl 9:77–85. https://doi.org/10.2351/1.4745447
37. Manvatkar VD, Gokhale AA, Jagan Reddy G, Venkataramana A, De A (2011) Estimation of melt pool dimensions, thermal cycle, and hardness distribution in the laser-engineered net shaping process of austenitic stainless steel. Metall and Mater Trans A 42:4080–4087. https://doi.org/10.1007/s11661-011-0787-8
38. van de Hulst H (2012) Light scattering by small particles. Dover Publications, USA
39. Atkins PW, De Paula J (2006) Atkins' physical chemistry. Oxford University Press, Oxford
40. Liu J, Li L, Zhang Y, Xie X (2005) Attenuation of laser power of a focused gaussian beam during interaction between a laser and powder in coaxial laser cladding. J Phys D Appl Phys 38:1546–1550. https://doi.org/10.1088/0022-3727/38/10/008
41. Lin J (1999) Concentration mode of the powder stream in coaxial laser cladding. Opt Laser Technol 31:251–257. https://doi.org/10.1016/s0030-3992(99)00049-3
42. Lin J (2000) Laser attenuation of the focused powder streams in coaxial laser cladding. J Laser Appl 12:28–33. https://doi.org/10.2351/1.521910
43. Pinkerton AJ, Li L (2002) A verified model of the behaviour of the axial powder stream concentration from a coaxial laser cladding nozzle. Int Congr Appl Lasers Electro-Opt 165528: 2002. https://doi.org/10.2351/1.5066174
44. Pinkerton AJ, Li L (2004) Modelling powder concentration distribution from a coaxial deposition nozzle for laser-based rapid tooling. J Manuf Sci Eng 126:33. https://doi.org/10.1115/1.1643748
45. Yang N (2009) Concentration model based on movement model of powder flow in coaxial laser cladding. Opt Laser Technol 41:94–98. https://doi.org/10.1016/j.optlastec.2008.03.008
46. Chew Y, Pang JHL, Bi G, Song B (2015) Thermo-mechanical model for simulating laser cladding induced residual stresses with single and multiple clad beads. J Mater Process Technol 224:89–101. https://doi.org/10.1016/j.jmatprotec.2015.04.031
47. Tan H, Zhang F, Fu X, Meng J, Hu G, Fan W, Huang W (2016) Development of powder flow model of laser solid forming by analysis method. Int J Adv Manuf Technol 82:1421–1431. https://doi.org/10.1007/s00170-015-7481-8
48. Wu J, Zhao P, Wei H, Lin Q, Zhang Y (2018) Development of powder distribution model of discontinuous coaxial powder stream in laser direct metal deposition. Powder Technol 340:449–458. https://doi.org/10.1016/j.powtec.2018.09.032
49. Stankevich SL, Topalov IK, Golovin PA, Valdaytseva EA (2018) Study of metallic powder flow in discrete coaxial nozzles. J Phys

Conf Ser 1109:012008. https://doi.org/10.1088/1742-6596/1109/1/012008
50. Frenk A, Vandyoussefi M, Wagnière JD, Kurz W, Zryd A (1997) Analysis of the laser-cladding process for stellite on steel. Metall and Mater Trans B 28:501–508. https://doi.org/10.1007/s11663-997-0117-0
51. Diniz Neto OO, Vilar R (2002) Physical-computational model to describe the interaction between a laser beam and a powder jet in laser surface processing. J Laser Appl 14:46–51. https://doi.org/10.2351/1.1436485
52. Fu Y, Loredo A, Martin B, Vannes AB (2002) A theoretical model for laser and powder particles interaction during laser cladding. J Mater Process Technol 128:106–112. https://doi.org/10.1016/s0924-0136(02)00433-8
53. Pinkerton AJ (2007) An analytical model of beam attenuation and powder heating during coaxial laser direct metal deposition. J Phys D Appl Phys 40:7323–7334. https://doi.org/10.1088/0022-3727/40/23/012
54. Qi H, Mazumder J, Ki H (2006) Numerical simulation of heat transfer and fluid flow in coaxial laser cladding process for direct metal deposition. J Appl Phys 024903:100. https://doi.org/10.1063/1.2209807
55. He X, Mazumder J (2007) Transport phenomena during direct metal deposition. J Appl Phys 053113:101. https://doi.org/10.1063/1.2710780
56. Liu Z, Qi H (2014) Numerical simulation of transport phenomena for a double-layer laser powder deposition of single-crystal superalloy. Metall and Mater Trans A 45:1903–1915. https://doi.org/10.1007/s11661-013-2178-9
57. Liu Z, Jiang L, Wang Z, Song L (2018) Mathematical modeling of transport phenomena in multi-track and multi-layer laser powder deposition of single-crystal superalloy. Metall and Mater Trans A 49:6533–6543. https://doi.org/10.1007/s11661-018-4914-7
58. Versteeg H, Malalasekera W (2007), An introduction to computational fluid dynamics: the finite volume method. Pearson Education Limited
59. Katinas C, Shang W, Shin YC, Chen J (2018) Modeling particle spray and capture efficiency for direct laser deposition using a four nozzle powder injection system. J Manuf Sci Eng 140:041014–041014–10. https://doi.org/10.1115/1.4038997
60. Shih TH, Liou WW, Shabbir A, Yang Z, Zhu J (1995) A new k-ϵ eddy viscosity model for high reynolds number turbulent flows. Comput Fluids 24:227–238. https://doi.org/10.1016/0045-7930(94)00032-T
61. Menter FR (1994) Two-equation eddy-viscosity turbulence models for engineering applications. AIAA J 32:1598–1605
62. Lin J (2000) Numerical simulation of the focused powder streams in coaxial laser cladding. J Mater Process Technol 105:17–23. https://doi.org/10.1016/s0924-0136(00)00584-7
63. Wen SY, Shin YC, Murthy JY, Sojka PE (2009) Modeling of coaxial powder flow for the laser direct deposition process. Int J Heat Mass Transfer 52:5867–5877. https://doi.org/10.1016/j.ijheatmasstransfer.2009.07.018
64. Zhu G, Li D, Zhang A, Tang Y (2011) Numerical simulation of metallic powder flow in a coaxial nozzle in laser direct metal deposition. Opt Laser Technol 43:106–113. https://doi.org/10.1016/j.optlastec.2010.05.012
65. Gosman AD, Ioannides E (1983) Aspects of computer simulation of liquid-fueled combustors. J Energy 7:482–490. https://doi.org/10.2514/3.62687
66. Morsi SA, Alexander AJ (1972) An investigation of particle trajectories in two-phase flow systems. J Fluid Mech 55:193–208. https://doi.org/10.1017/S0022112072001806
67. Haider A, Levenspiel O (1989) Drag coefficient and terminal velocity of spherical and nonspherical particles. Powder Technol 58:63–70. https://doi.org/10.1016/0032-5910(89)80008-7
68. Chein R, Chung JN (1988) Simulation of particle dispersion in a two-dimensional mixing layer. AIChE J 34:946–954. https://doi.org/10.1002/aic.690340607
69. Ranz WE, Marshall Jr W R (1952a) Evaporation from drops, part i. Chem Eng Prog 48:141–146
70. Ranz WE, Marshall JrWR (1952b) Evaporation from drops, part ii. Chem Eng Prog 48:173–180
71. Zhang A, Li D, Zhou Z, Zhu G, Lu B (2010) Numerical simulation of powder flow field on coaxial powder nozzle in laser metal direct manufacturing. Int J Adv Manuf Technol 49:853–859. https://doi.org/10.1007/s00170-010-2657-8
72. ANSYS, Inc (2019) ANSYS® Academic Research Fluent, Release 19 2
73. Bedenko DV, Gulaiev IP, Gurin AM, Kovalev OB, Pinaev PA, Sergachev DV, Smirnov AL (2018) Modelling of gas-powder transportation during coaxial laser cladding. AIP Conf Proc 2027:030109. https://doi.org/10.1063/1.5065203
74. Pan H, Liou F (2005) Numerical simulation of metallic powder flow in a coaxial nozzle for the laser aided deposition process. J Mater Process Technol 168:230–244. https://doi.org/10.1016/j.jmatprotec.2004.11.017
75. Pan H, Landers RG, Liou F (2006) Dynamic modeling of powder delivery systems in gravity-fed powder feeders. J Manuf Sci Eng 128:337–345. https://doi.org/10.1115/1.2120778
76. Pan H, Sparks T, Thakar YD, Liou F (2005) The investigation of gravity-driven metal powder flow in coaxial nozzle for laser-aided direct metal deposition process. J Manuf Sci Eng 128:541–553. https://doi.org/10.1115/1.2162588
77. Polyanskiy TA, Zaitsev AV, Gulyaev IP, Gurin AM (2018) Numerical and experimental investigation of two phase flow for direct metal deposition. Journal of Physics: Conference Series: 1109. https://doi.org/10.1088/1742-6596/1109/1/012010
78. Zekovic S, Dwivedi R, Kovacevic R (2007) Numerical simulation and experimental investigation of gas–powder flow from radially symmetrical nozzles in laser-based direct metal deposition. Int J Mach Tools Manuf 47:112–123. https://doi.org/10.1016/j.ijmachtools.2006.02.004
79. Zhu G, Li D, Zhang A, Pi G, Tang Y (2011) The influence of standoff variations on the forming accuracy in laser direct metal deposition. Rapid Prototyp J 17:98–106. https://doi.org/10.1108/13552541111113844
80. Kovalev OB, Zaitsev AV, Novichenko D, Smurov I (2011) Theoretical and experimental investigation of gas flows, powder transport and heating in coaxial laser direct metal deposition (dmd) process. J Therm Spray Tech 20:465–478. https://doi.org/10.1007/s11666-010-9539-3
81. Liu H, Hao J, Yu G, Yang H, Wang L, Han Z (2016) A numerical study on metallic powder flow in coaxial laser cladding. J Appl Fluid Mech 9:2247–2256
82. Liu CY, Lin J (2003) Thermal processes of a powder particle in coaxial laser cladding. Opt Laser Technol 35:81–86. https://doi.org/10.1016/s0030-3992(02)00145-7
83. Ibarra-Medina J, Pinkerton AJ (2010) A cfd model of the laser, coaxial powder stream and substrate interaction in laser cladding. Phys Procedia 5:337–346. https://doi.org/10.1016/j.phpro.2010.08.060
84. Ibarra-Medina J, Pinkerton AJ (2011) Numerical investigation of powder heating in coaxial laser metal deposition. Surf Eng 27:754–761. https://doi.org/10.1179/1743294411y.0000000017
85. Tabernero I, Lamikiz A, Ukar E, López de Lacalle LN, Angulo C, Urbikain G (2010) Numerical simulation and experimental validation of powder flux distribution in coaxial laser cladding. J Mater Process Technol 210:2125–2134. https://doi.org/10.1016/j.jmatprotec.2010.07.036
86. Tabernero I, Lamikiz A, Martínez S, Ukar E, López de Lacalle LN (2012) Modelling of energy attenuation due to powder

flow-laser beam interaction during laser cladding process. J Mater Process Technol 212:516–522. https://doi.org/10.1016/j.jmatprotec.2011.10.019
87. Devesse W, De Baere D, Guillaume P (2015) Modeling of laser beam and powder flow interaction in laser cladding using ray-tracing. J Laser Appl 27:S29208. https://doi.org/10.2351/1.4906394
88. El Cheikh H, Courant B, Hascoët JY, Guillén R (2012a) Prediction and analytical description of the single laser track geometry in direct laser fabrication from process parameters and energy balance reasoning. J Mater Process Technol 212:1832–1839. https://doi.org/10.1016/j.jmatprotec.2012.03.016
89. El Cheikh H, Courant B, Branchu S, Hascoët JY, Guillén R (2012b) Analysis and prediction of single laser tracks geometrical characteristics in coaxial laser cladding process. Opt Lasers Eng 50:413–422. https://doi.org/10.1016/j.optlaseng.2011.10.014
90. El Cheikh H, Courant B, Branchu S, Huang X, Hascoët JY, Guillén R (2012c) Direct laser fabrication process with coaxial powder projection of 316l steel. geometrical characteristics and microstructure characterization of wall structures. Opt Lasers Eng 50:1779–1784. https://doi.org/10.1016/j.optlaseng.2012.07.002
91. Labudovic M, Hu D, Kovacevic R (2003) A three dimensional model for direct laser metal powder deposition and rapid prototyping. J Mater Sci 38:35–49. https://doi.org/10.1023/a:1021153513925
92. de Oliveira U, Ocelík V, De Hosson JTM (2005) Analysis of coaxial laser cladding processing conditions. Surf Coat Technol 197:127–136. https://doi.org/10.1016/j.surfcoat.2004.06.029
93. Jouvard J, Grevey DF, Lemoine F, Vannes AB (1997) Continuous wave nd:yag laser cladding modeling: a physical study of track creation during low power processing. J Laser Appl 9:43–50. https://doi.org/10.2351/1.4745444
94. Fathi A, Toyserkani E, Khajepour A, Durali M (2006) Prediction of melt pool depth and dilution in laser powder deposition. J Phys D Appl Phys 39:2613–2623. https://doi.org/10.1088/0022-3727/39/12/022
95. Lalas C, Tsirbas K, Salonitis K, Chryssolouris G (2007) An analytical model of the laser clad geometry. Int J Adv Manuf Technol 32:34–41. https://doi.org/10.1007/s00170-005-0318-0
96. Partes K (2009) Analytical model of the catchment efficiency in high speed laser cladding. Surf Coat Technol 204:366–371. https://doi.org/10.1016/j.surfcoat.2009.07.041
97. Pinkerton AJ, Li L (2004) Modelling the geometry of a moving laser melt pool and deposition track via energy and mass balances. J Phys D Appl Phys 37:1885–1895. https://doi.org/10.1088/0022-3727/37/14/003
98. Zhou S, Dai X, Zheng H (2011) Analytical modeling and experimental investigation of laser induction hybrid rapid cladding for ni-based wc composite coatings. Opt Laser Technol 43:613–621. https://doi.org/10.1016/j.optlastec.2010.09.001
99. Ahsan MN, Pinkerton AJ (2011) An analytical-numerical model of laser direct metal deposition track and microstructure formation. Model Simul Mater Sci Eng 19:055003
100. Cline HE, Anthony TR (1977) Heat treating and melting material with a scanning laser or electron beam. J Appl Phys 48:3895–3900. https://doi.org/10.1063/1.324261
101. Wang Q, Li J, Gouge M, Nassar AR, Michaleris P, Reutzel EW (2016) Physics-based multivariable modeling and feedback linearization control of melt-pool geometry and temperature in directed energy deposition. J Manuf Sci Eng 139:021013–021013–12. https://doi.org/10.1115/1.4034304
102. Chaskalovic J (2008) Finite element methods for engineering sciences: theoretical approach and problem solving techniques. Springer, Berlin
103. Li J, Wang Q, Michaleris P, Reutzel EW, Nassar AR (2017) An extended lumped-parameter model of melt-pool geometry to predict part height for directed energy deposition. J Manuf Sci Eng 139:091016–091016–14. https://doi.org/10.1115/1.4037235
104. Rosenthal D (1946) The theory of moving sources of heat and its application of metal treatments. Trans ASME 68:849–866
105. Carslaw H, Jaeger J (1959) Conduction of heat in solids. Oxford University Press, Oxford
106. Rykalin N, Uglov A, Kokora A (1978) Laser machining and welding. Mir Publishers, Moscow
107. Elsen MV, Baelmans M, Mercelis P, Kruth JP (2007) Solutions for modelling moving heat sources in a semi-infinite medium and applications to laser material processing. Int J Heat Mass Transfer 50(23):4872–4882. https://doi.org/10.1016/j.ijheatmasstransfer.2007.02.044
108. Pinkerton AJ, Li L (2004) The significance of deposition point standoff variations in multiple-layer coaxial laser cladding (coaxial cladding standoff effects). Int J Mach Tools Manuf 44:573–584. https://doi.org/10.1016/j.ijmachtools.2004.01.001
109. Li J, Wang Q, Michaleris P (2018) An analytical computation of temperature field evolved in directed energy deposition. J Manuf Sci Eng 140:101004–101004–13. https://doi.org/10.1115/1.4040621
110. Tan H, Chen J, Zhang F, Lin X, Huang W (2010) Process analysis for laser solid forming of thin-wall structure. Int J Mach Tools Manuf 50:1–8. https://doi.org/10.1016/j.ijmachtools.2009.10.003
111. Ning J, Sievers DE, Garmestani H, Liang SY (2019) Analytical modeling of transient temperature in powder feed metal additive manufacturing during heating and cooling stages. Appl Phys A 125:496. https://doi.org/10.1007/s00339-019-2782-7
112. Huang Y, Khamesee MB, Toyserkani E (2019) A new physics-based model for laser directed energy deposition (powder-fed additive manufacturing): from single-track to multi-track and multi-layer. Opt Laser Technol 109:584–599. https://doi.org/10.1016/j.optlastec.2018.08.015
113. Ocelík V, Nenadl O, Palavra A, Hosson JD (2014) On the geometry of coating layers formed by overlap. Surf Coat Technol 242:54–61. https://doi.org/10.1016/j.surfcoat.2014.01.018
114. Schiaffino S, Sonin AA (1997) Molten droplet deposition and solidification at low weber numbers. Phys Fluids 9:3172–3187. https://doi.org/10.1063/1.869434
115. Michaleris P (2014) Modeling metal deposition in heat transfer analyses of additive manufacturing processes. Finite Elem Anal Des 86:51–60. https://doi.org/10.1016/j.finel.2014.04.003
116. Wang L, Felicelli S, Gooroochurn Y, Wang P, Horstemeyer M (2006) Numerical simulation of the temperature distribution and solid phase evolution in the LENS™process. Proceedings of the Solid Freeform Fabrication Symposium, pp 453–463
117. ESI Group (2019) SYSWELD 2019
118. Wang L, Felicelli S (2007a) Influence of process parameters on the phase transformation and consequent hardness induced by the LENS™process. Proceedings of TMS Conference, pp 63–72
119. Wang L, Felicelli S (2007b) Process modeling in laser deposition of multilayer SS410 steel. J Manuf Sci Eng 129:1028–1034. https://doi.org/10.1115/1.2738962
120. Wang L, Felicelli SD, Craig JE (2007) Thermal modeling and experimental validation in the LENS™process. Proceedings of the Solid Freeform Fabrication Symposium, pp 100–111
121. Wang L, Felicelli S, Gooroochurn Y, Wang PT, Horstemeyer MF (2008a) Optimization of the LENS® process for steady molten pool size. Mater Sci Eng A 474:148–156. https://doi.org/10.1016/j.msea.2007.04.119
122. Wang L, Felicelli SD, Pratt P (2008b) Residual stresses in LENS-deposited AISI 410 Stainless Steel plates. Mater Sci Eng A 496:234–241. https://doi.org/10.1016/j.msea.2008.05.044

123. Ye R, Smugeresky JE, Zheng B, Zhou Y, Lavernia EJ (2006) Numerical modeling of the thermal behavior during the LENS® process. Mater Sci Eng A 428:47–53. https://doi.org/10.1016/j.msea.2006.04.079
124. Yin H, Wang L, Felicelli SD (2008) Comparison of two-dimensional and three-dimensional thermal models of the LENS® process. J Heat Transfer 130:102101–102101–7. https://doi.org/10.1115/1.2953236
125. Wang L, Felicelli S (2006) Analysis of thermal phenomena in LENS™deposition. Mater Sci Eng A 435-436:625–631. https://doi.org/10.1016/j.msea.2006.07.087
126. Hofmeister W, Wert M, Smugeresky J, Philliber JA, Griffith M, Ensz M (1999) Investigating solidification with the laser-engineered net shaping (LENS™) process. JOM 51:1–6
127. Patel CP, Patel R (2012) 3D heat transfer analysis and numerical modeling of LENS™process for thin wall by using Stainless Steel 304. Int J Modern Eng Res 2:1596–1601
128. Yang Q, Zhang P, Cheng L, Min Z, Chyu M, To AC (2016) Finite element modeling and validation of thermomechanical behavior of Ti-6Al-4V in directed energy deposition additive manufacturing. Add Manuf 12:169–177. https://doi.org/10.1016/j.addma.2016.06.012
129. Goldak J, Chakravarti A, Bibby M (1984) A new finite element model for welding heat sources. Metall Trans B 15:299–305. https://doi.org/10.1007/BF02667333
130. Shah K, Khurshid H, ul Haq I, Anwar S, Shah SA (2018) Numerical modelling of pulsed and continuous wave direct laser deposition of Ti-6Al-4V and Inconel 718. Int J Adv Manuf Technol 95:847–860. https://doi.org/10.1007/s00170-017-1224-y
131. Lampa C, Kaplan AFH, Powell J, Magnusson C (1997) An analytical thermodynamic model of laser welding. J Phys D Appl Phys 30:1293–1299. https://doi.org/10.1088/0022-3727/30/9/004
132. Lee WS, Yeh GW (1997) The plastic deformation behaviour of AISI 4340 alloy steel subjected to high temperature and high strain rate loading conditions. J Mater Process Technol 71:224–234. https://doi.org/10.1016/S0924-0136(97)00079-4
133. Yan L, Li W, Chen X, Zhang Y, Newkirk J, Liou F, Dietrich D (2017) Simulation of cooling rate effects on ti-48al-2cr-2nb crack formation in direct laser deposition. JOM 69:586–591. https://doi.org/10.1007/s11837-016-2211-8
134. Yan L, Zhang Y, Liou F (2018) A conceptual design of residual stress reduction with multiple shape laser beams in direct laser deposition. Finite Elem Anal Des 144:30–37. https://doi.org/10.1016/j.finel.2018.02.004
135. Khanafer K, Al-Masri A, Aithal S, Deiab I (2019) Multiphysics modeling and simulation of laser additive manufacturing process. Int J Interact Des Manuf (IJIDeM) 13:537–544. https://doi.org/10.1007/s12008-018-0520-6
136. Gouge MF, Heigel JC, Michaleris P, Palmer TA (2015) Modeling forced convection in the thermal simulation of laser cladding processes. Int J Adv Manuf Technol 79:307–320. https://doi.org/10.1007/s00170-015-6831-x
137. Heigel JC, Michaleris P, Reutzel EW (2015) Thermo-mechanical model development and validation of directed energy deposition additive manufacturing of ti–6al–4v. Add Manuf 5:9–19. https://doi.org/10.1016/j.addma.2014.10.003
138. Toyserkani E, Khajepour A, Corbin S (2004) 3-d finite element modeling of laser cladding by powder injection: effects of laser pulse shaping on the process. Opt Lasers Eng 41:849–867. https://doi.org/10.1016/s0143-8166(03)00063-0
139. Costa L, Vilar R, Réti T, Colaço R, Deus A, Felde I (2005a) Simulation of phase transformations in steel parts produced by laser powder deposition. Mater Sci Forum 473:315–320
140. Costa L, Vilar R, Reti T, Deus AM (2005b) Rapid tooling by laser powder deposition: process simulation using finite element analysis. Acta Mater 53:3987–3999. https://doi.org/10.1016/j.actamat.2005.05.003
141. Qian L, Mei J, Liang J, Wu X (2005) Influence of position and laser power on thermal history and microstructure of direct laser fabricated ti–6al–4v samples. Mater Sci Technol 21:597–605. https://doi.org/10.1179/174328405x21003
142. Neela V, De A (2009) Three-dimensional heat transfer analysis of LENS™process using finite element method. Int J Adv Manuf Technol 45:935–943. https://doi.org/10.1007/s00170-009-2024-9
143. Mahapatra MM, Li L (2012) Modeling of pulsed-laser superalloy powder deposition using moving distributed heat source. EPD Congress, pp 113–120. https://doi.org/10.1002/9781118359341.ch13
144. Marimuthu S, Clark D, Allen J, Kamara A, Mativenga P, Li L, Scudamore R (2013) Finite element modelling of substrate thermal distortion in direct laser additive manufacture of an aero-engine component. Proc Inst Mech Eng Part C J Mech Eng Sci 227:1987–1999. https://doi.org/10.1177/0954406212470363
145. Sammons PM, Bristow DA, Landers RG (2013) Height dependent laser metal deposition process modeling. J Manuf Sci Eng 135:054501–054501–7. https://doi.org/10.1115/1.4025061
146. Amine T, Newkirk JW, Liou F (2014a) Investigation of effect of process parameters on multilayer builds by direct metal deposition. Appl Therm Eng 73:500–511. https://doi.org/10.1016/j.applthermaleng.2014.08.005
147. Amine T, Newkirk JW, Liou F (2014b) An investigation of the effect of direct metal deposition parameters on the characteristics of the deposited layers. Case Stud Therm Eng 3:21–34. https://doi.org/10.1016/j.csite.2014.02.002
148. Hochmann EA, Salehinia I (2018) How convection on the substrate affects the thermal history of the build in direct laser deposition-finite element analysis. Int J Adv Manuf Technol 96:3471–3480. https://doi.org/10.1007/s00170-018-1696-4
149. Walker TR, Bennett CJ, Lee TL, Clare AT (2019) A validated analytical-numerical modelling strategy to predict residual stresses in single-track laser deposited in718. Int J Mech Sci 151:609–621. https://doi.org/10.1016/j.ijmecsci.2018.12.004
150. Denlinger ER, Michaleris P (2016) Effect of stress relaxation on distortion in additive manufacturing process modeling. Add Manuf 12:51–59. https://doi.org/10.1016/j.addma.2016.06.011
151. Wang Z, Denlinger E, Michaleris P, Stoica AD, Ma D, Beese AM (2017) Residual stress mapping in Inconel 625 fabricated through additive manufacturing: method for neutron diffraction measurements to validate thermomechanical model predictions. Mater Des 113:169–177. https://doi.org/10.1016/j.matdes.2016.10.003
152. Peyre P, Aubry P, Fabbro R, Neveu R, Longuet A (2008) Analytical and numerical modelling of the direct metal deposition laser process. J Phys D Appl Phys 025403:41. https://doi.org/10.1088/0022-3727/41/2/025403
153. Kumar S, Roy S (2008) Development of a theoretical process map for laser cladding using two-dimensional conduction heat transfer model. Comput Mater Sci 41:457–466. https://doi.org/10.1016/j.commatsci.2007.05.002
154. Hofman JT, de Lange DF, Pathiraj B, Meijer J (2011) Fem modeling and experimental verification for dilution control in laser cladding. J Mater Process Technol 211:187–196. https://doi.org/10.1016/j.jmatprotec.2010.09.007
155. Hofman JT (2009) Development of an observation and control system for industrial laser cladding. PhD thesis, University of Twente, Netherlands
156. Birnbaum A, Michopoulos JG, Iliopoulos AP (2016) Simulating geometric and thermal aspects of powder-jet laser additive manufacturing. ASME 2016 International Design Engineering Technical Conferences and Computers and Information in Engineering Conference, pp V01AT02A034–V01AT02A034

157. Hirt C, Amsden A, Cook J (1974) An arbitrary Lagrangian-Eulerian computing method for all flow speeds. J Comput Phys 14:227–253. https://doi.org/10.1016/0021-9991(74)90051-5
158. Bedenko DV, Kovalev OB, Smurov I, Zaitsev AV (2016) Numerical simulation of transport phenomena, formation the bead and thermal behavior in application to industrial dmd technology. Int J Heat Mass Transfer 95:902–912. https://doi.org/10.1016/j.ijheatmasstransfer.2015.12.046
159. Bedenko DV, Kovalev OB (2013) Modelling of heat and mass transfer in the laser cladding during direct metal deposition. Thermophys Aeromech 20:251–261. https://doi.org/10.1134/S086986431302011X
160. Tseng YH, Ferziger JH (2003) A ghost-cell immersed boundary method for flow in complex geometry. J Comput Phys 192:593–623. https://doi.org/10.1016/j.jcp.2003.07.024
161. Bennon W, Incropera F (1987a) A continuum model for momentum, heat and species transport in binary solid-liquid phase change systems-i. model formulation. Int J Heat Mass Transfer 30:2161–2170. https://doi.org/10.1016/0017-9310(87)90094-9
162. Bennon W, Incropera F (1987b) A continuum model for momentum, heat and species transport in binary solid-liquid phase change systems-ii. application to solidification in a rectangular cavity. Int J Heat Mass Transfer 30:2171–2187. https://doi.org/10.1016/0017-9310(87)90095-0
163. Osher S, Fedkiw R (2003) Level set methods and dynamic implicit surfaces. Springer, Berlin
164. Sethian JA, Smereka P (2003) Level set methods for fluid interfaces. Ann Rev Fluid Mech 35:341–372. https://doi.org/10.1146/annurev.fluid.35.101101.161105
165. Han L, Liou FW (2004) Numerical investigation of the influence of laser beam mode on melt pool. Int J Heat Mass Transfer 47:4385–4402. https://doi.org/10.1016/j.ijheatmasstransfer.2004.04.036
166. Han L, Liou FW, Musti S (2005a) Thermal behavior and geometry model of melt pool in laser material process. J Heat Transf 127:1005–1014. https://doi.org/10.1115/1.2005275
167. Han L, Phatak KM, Liou FW (2005b) Modeling of laser deposition and repair process. J Laser Appl 17:89–99. https://doi.org/10.2351/1.1848523
168. He X, Yu G, Mazumder J (2010) Temperature and composition profile during double-track laser cladding of h13 tool steel. J Phys D Appl Phys 015502:43. https://doi.org/10.1088/0022-3727/43/1/015502
169. Lee D, Mazumder J (2016) Effects of laser beam spatial distribution on laser-material interaction. Journal of Laser Applications 032003:28. https://doi.org/10.2351/1.4947096
170. Li S, Xiao H, Liu K, Xiao W, Li Y, Han X, Mazumder J, Song L (2017) Melt-pool motion, temperature variation and dendritic morphology of Inconel 718 during pulsed- and continuous-wave laser additive manufacturing: a comparative study. Mater Des 119:351–360. https://doi.org/10.1016/j.matdes.2017.01.065
171. Hirt C, Nichols B (1981) Volume of fluid (VOF) method for the dynamics of free boundaries. J Comput Phys 39:201–225. https://doi.org/10.1016/0021-9991(81)90145-5
172. Morville S, Carin M, Peyre P, Gharbi M, Carron D, Le Masson P, Fabbro R (2012) 2D longitudinal modeling of heat transfer and fluid flow during multilayered direct laser metal deposition process. J Laser Appl 24:032008. https://doi.org/10.2351/1.4726445
173. Gan Z, Yu G, He X, Li S (2017) Numerical simulation of thermal behavior and multicomponent mass transfer in direct laser deposition of co-base alloy on steel. Int J Heat Mass Transfer 104:28–38. https://doi.org/10.1016/j.ijheatmasstransfer.2016.08.049
174. Song J, Chew Y, Bi G, Yao X, Zhang B, Bai J, Moon SK (2018) Numerical and experimental study of laser aided additive manufacturing for melt-pool profile and grain orientation analysis. Mater Des 137:286–297. https://doi.org/10.1016/j.matdes.2017.10.033
175. Lee Y, Nordin M, Babu S, Farson DF (2014) Influence of fluid convection on weld pool formation in laser cladding. Weld J 93:292S–300S
176. Lee Y, Farson DF (2015) Surface tension-powered build dimension control in laser additive manufacturing process. Int J Adv Manuf Technol 85:1035–1044. https://doi.org/10.1007/s00170-015-7974-5
177. Lee Y, Farson DF (2016) Simulation of transport phenomena and melt pool shape for multiple layer additive manufacturing. J Laser Appl 28:012006. https://doi.org/10.2351/1.4935711
178. Dubrov AV, Mirzade FK, Dubrov VD, Panchenko VY (2018) Heat transfer and thermocapillary convection during the laser deposition of metal powders implemented in additive technologies. Journal of Surface Investigation: X-ray. Synchrotron Neutron Techn 12:54–63. https://doi.org/10.1134/s1027451018010081
179. Vásquez F, Ramos-Grez JA, Walczak M (2012) Multiphysics simulation of laser-material interaction during laser powder depositon. Int J Adv Manuf Technol 59:1037–1045. https://doi.org/10.1007/s00170-011-3571-4
180. Sankaranarayanan S, Kar A (1999) Nonlinear effects of laser-plasma interaction on melt-surface temperature. J Phys D Appl Phys 32:777–784. https://doi.org/10.1088/0022-3727/32/7/005
181. Manvatkar V, De A, DebRoy T (2014) Heat transfer and material flow during laser assisted multi-layer additive manufacturing. J Appl Phys 124905:116. https://doi.org/10.1063/1.4896751
182. Manvatkar V, De A, DebRoy T (2015) Spatial variation of melt pool geometry, peak temperature and solidification parameters during laser assisted additive manufacturing process. Mater Sci Technol 31:924–930. https://doi.org/10.1179/1743284714y.0000000701
183. Mukherjee T, Zhang W, DebRoy T (2017) An improved prediction of residual stresses and distortion in additive manufacturing. Comput Mater Sci 126:360–372. https://doi.org/10.1016/j.commatsci.2016.10.003
184. Mukherjee T, Zuback JS, Zhang W, DebRoy T (2018) Residual stresses and distortion in additively manufactured compositionally graded and dissimilar joints. Comput Mater Sci 143:325–337. https://doi.org/10.1016/j.commatsci.2017.11.026
185. Wen S, Shin YC (2010) Modeling of transport phenomena during the coaxial laser direct deposition process. J Appl Phys 044908:108. https://doi.org/10.1063/1.3474655
186. De A, Debroy T (2005) Reliable calculations of heat and fluid flow during conduction mode laser welding through optimization of uncertain parameters. Weld J 84:101–112
187. Peng X, Lin X, Lee D, Yan Y, Wang B (2001) Effects of initial molten pool and marangoni flow on solid melting. Int J Heat Mass Transfer 44:457–470. https://doi.org/10.1016/S0017-9310(00)00070-3
188. Wen S, Shin YC (2010) Modeling of the off-axis high power diode laser cladding process. J Heat Transfer 133:031007–031007–10. https://doi.org/10.1115/1.4002447
189. Wen S, Shin YC (2011a) Comprehensive predictive modeling and parametric analysis of multitrack direct laser deposition processes. J Laser Appl 23:022003. https://doi.org/10.2351/1.3567962
190. Wen S, Shin YC (2011b) Modeling of transport phenomena in direct laser deposition of metal matrix composite. Int J Heat Mass Transfer 54:5319–5326. https://doi.org/10.1016/j.ijheatmasstransfer.2011.08.011
191. Katinas C, Liu S, Shin YC (2018) Self-sufficient modeling of single track deposition of Ti-6Al-4V with the prediction of capture efficiency. J Manuf Sci Eng 141:011001–011001–10. https://doi.org/10.1115/1.4041423

192. ANSYS, Inc (2019) ANSYS® Academic Research CFX, Release 19, 2
193. Flow Science, Inc (2019) FLOW-3D®, Version 12, 0
194. Maitre E (2006) Review of numerical methods for free interfaces. Les Houches 27:31
195. Gibou F, Fedkiw R, Osher S (2018) A review of level-set methods and some recent applications. J Comput Phys 353:82–109. https://doi.org/10.1016/j.jcp.2017.10.006
196. Donea J, Huerta A, Ponthot JP, Rodríguez-ferran A (2004) Arbitrary Lagrangian-Eulerian methods. In: Encyclopedia of Computational Mechanics. Wiley. https://doi.org/10.1002/0470091355.ecm009
197. Bishop CM (2006) Pattern recognition and machine learning (information science and statistics). Springer, Berlin
198. Kamath C (2016) Data mining and statistical inference in selective laser melting. Int J Adv Manuf Technol 86:1659–1677. https://doi.org/10.1007/s00170-015-8289-2
199. Zohdi TI (2019) Electrodynamic machine-learning-enhanced fault-tolerance of robotic free-form printing of complex mixtures. Comput Mech 63:913–929. https://doi.org/10.1007/s00466-018-1629-y